Ocean-Cloud-Atmosphere-Land Interactions in the Southeastern Pacific: The VOCALS Program

C. R. Mechoso[1], R. Wood[2], R. Weller[3], C. S. Bretherton[2], A. D. Clarke[4], H. Coe[5], C. Fairall[6], J. T. Farrar[3], G. Feingold[6], R. Garreaud[7], C. Grados[8], J. C. McWilliams[1], S. P. de Szoeke[9], S. E. Yuter[10], and P. Zuidema[11]

[1]Department of Atmospheric and Oceanic Sciences, University of California, Los Angeles, USA
[2]Department of Atmospheric Sciences, University of Washington, Seattle, USA
[3]Department of Physical Oceanography, Woods Hole Oceanographic Institution, Woods Hole, USA
[4]Department of Oceanography, University of Hawai`i at Manoa, Honolulu, USA
[5]School of Earth, Atmospheric and Environmental Sciences, University of Manchester, United Kingdom
[6]NOAA Earth System Research Laboratory, Boulder, USA
[7]Department of Geophysics, Universidad de Chile & Center for Climate and Resilience Research, Universidad de Chile
[8]Instituto del Mar del Perú (IMARPE), Circuito-Callao, Perú
[9]College of Earth, Ocean, and Atmospheric Sciences, Oregon State University, Corvallis, USA
[10]Department of Marine, Earth and Atmospheric Sciences, North Carolina State University, Raleigh, USA
[11]University of Miami/Rosenstiel School of Marine and Atmospheric Science, Miami, FL

Corresponding autor: Carlos R. Mechoso
Department of Atmospheric and Oceanic Sciences
University of California, Los Angeles
Los Angeles, CA 90095, USA
ph: 310-825-3057
Email: mechoso@atmos.ucla.edu

Abstract

The present paper describes the VAMOS Ocean-Cloud-Atmosphere-Land Study (VOCALS), an international research program focused upon improved understanding and modeling of the southeastern Pacific (SEP) climate system on diurnal to interannual timescales. In the framework of the SEP climate, VOCALS has been addressing two fundamental objectives: 1) improved simulations with coupled atmosphere-ocean general circulation models (CGCMs) with an emphasis on reducing systematic errors in the region, and 2) improved estimates of the indirect effects of aerosols on low clouds and climate, with an emphasis on a more precise quantification of those effects. VOCALS major scientific activities are outlined, and selected achievements are highlighted. Activities described include monitoring, a large international field campaign (the VOCALS Regional Experiment), and two model assessments. The program has produced significant advances in the understanding of major issues in the SEP: the coastal circulation and the diurnal cycle, the ocean heat budget, factors controlling precipitation and formation and formation of pockets of open cells in the stratocumulus decks, aerosol impacts on clouds, and estimation of the first aerosol indirect effect. The paper concludes with a brief presentation on VOCALS contribution to capacity building before a summary of current activities, science findings and remaining questions.

Capsule: New focused measurements, analyses, and modeling of the Southeast Pacific climate system are helping to improve our understanding of the atmospheric and oceanic processes and their interactions in the eastern tropical ocean regions.

1. Introduction

The VAMOS[1] Ocean-Cloud-Atmosphere-Land Study (VOCALS) is an international research program focused upon improved understanding and modeling of the southeastern Pacific (SEP) climate system on diurnal to interannual timescales. The SEP is very important in many ways: It produces nearly a fifth of the global fish catch (UNEP 2005) and variations in its climate can have global reach through teleconnections and aerosol indirect effects.

The SEP is characterized by strong coastal ocean upwelling, the coldest sea surface temperatures (SSTs) at comparable latitudes, the planet's most extensive subtropical stratocumulus deck, and a high and steep cordillera to the east (Fig. 1). The regional climate is defined by strong interactions between the ocean, atmosphere, land, clouds, and aerosol particles, providing extraordinary challenges to numerical simulations and model-based predictions of climate variability and change. Anthropogenic emissions of pollutants along the Chilean and Peruvian coasts enter otherwise extremely pristine air masses over the Pacific Ocean, providing extreme spatial contrasts in aerosol and cloud microphysical properties. A deeper and broader understanding of the physical-chemical processes that shape such a complex climate system is invaluable and will provide guidance on how these processes may be better represented in numerical models. In the framework of the SEP climate, VOCALS has been addressing two fundamental objectives: 1) improved simulations with coupled atmosphere-ocean general circulation models (CGCMs) with an emphasis on reducing systematic errors in the region (Mechoso et al. 1995; Davey et al. 2001; de Szoeke et al. 2008), and 2) improved estimates of

[1] VAMOS stands for Variability of the American Monsoon Systems, a panel of the World Climate Research Programme (WCRP)/Climate Variability Programme (CLIVAR). VOCALS researchers acknowledge the community that originated and nurtured the program.

90 the indirect effects of aerosols on low clouds and climate, with an emphasis on a more precise
91 quantification of those effects (Lohmann and Feichter 2005; Quaas et al. 2009).

92 The VOCALS program builds on a solid bedrock of knowledge about the SEP climate,
93 its variability, and the global impacts of such variability (Mechoso and Wood 2010). The
94 program followed the Eastern Pacific Investigation of Climate (EPIC), which investigated the
95 Intertropical Convergence Zone (ITCZ)/cold-tongue complex and marine boundary layer (MBL)
96 clouds over the SEP (Bretherton et al. 2004). An instrumented mooring installed during EPIC in
97 October 2000 at 20°S, 85°W by the Woods Hole Oceanographic Institution (hereafter the WHOI
98 buoy; Colbo and Weller 2007; 2009) has monitored for over a decade the diurnal to interannual
99 variability of regional meteorology, clouds, and upper ocean structure. A second mooring
100 maintained by the Chilean Navy Hydrographic and Oceanographic Service close to (20°S,
101 75°W) (hereafter the SHOA buoy) collected data for two years with additional instrumentation
102 added by WHOI. Annual buoy-tending cruises drove opportunities for shipborne atmospheric
103 and ocean sampling (e.g., Tomlinson et al. 2007; Serpetzoglou et al. 2008; Zuidema et al. 2009;
104 de Szoeke et al. 2010; and references therein). Other cruises and field campaigns organized in
105 the region with invaluable participation from scientists from Chile and Peru had provided unique
106 context on the coastal atmospheric and ocean circulations (e.g., the CIMAR-5 cruise, Garreaud et
107 al. 2001; Painemal et al. 2010). VOCALS also builds on an important body of modeling work on
108 the SEP climate. It is widely recognized that clouds in the subsiding regions of the eastern
109 tropical oceans drive uncertainty in climate sensitivity simulated by numerical models (Bony and
110 Dufresne 2005). In the specific context of the eastern Pacific climate, it is known that
111 stratocumulus cloud decks are essential for key features such as the asymmetry about the equator
112 and annual cycle dominated by the semi-annual component (Philander et al. 1996; Ma et al.

1996; Yu and Mechoso 1999a,b; Zhang et al. 2005). Satellite data and the first cloud-focused research cruise over the SEP also indicated that the clouds are typified by extremely strong gradients in the concentration of cloud droplets (Bretherton et al. 2004; Bennartz 2007) and that these gradients could to drive major impacts on the radiative budget of the region. VOCALS is also informed from the knowledge that the SEP stratocumulus deck is frequently punctuated by regions of open cellular convection that had been termed Pockets of Open Cells (POCs, Stevens et al. 2005). The transition from closed to open cells driving POC formation appeared to be driven by processes internal to the MBL (Wood and Hartmann 2006). It was also recognized that stratocumulus cloud albedo is sensitive to both natural and anthropogenic atmospheric aerosols (Twomey et al. 1974, 1977), both of which are produced in the SEP by desert dust, copper smelters (Huneeus et al. 2006) and urban areas.

Despite such an impressive background, major gaps in the knowledge of the SEP climate remained, which motivated the VOCALS program. Sea surface temperatures (SSTs) simulated by CGCMs were too warm by ~2-4 K and cloudiness was too low by ~50% (e.g., Ma et al. 1996). Reducing those errors required additional data for model validation and development. The WHOI buoy had started to produce clues that required further exploration. The buoy data showed that the mean surface fluxes of heat and freshwater in the SEP act to make the surface waters warmer and saltier, but the mean ocean circulation, including geostrophic and Ekman transport and upwelling, appeared insufficient to balance those fluxes (Colbo and Weller 2007). Furthermore, research on marine low clouds was (still is) desperately needed to overcome the CGCMs difficulties with their simulation and improve quantification of the Earth's climate sensitivity. Most climate models represent these indirect effects of aerosols (AIEs) on climate, but their magnitude differs widely across models (Lohmann and Feichter 2005; Quaas et al.

2009). Key issues hampering better quantification of AIEs center upon the impacts of aerosols on precipitation and cloud mesoscale organization, the transport of continental aerosols to the remote ocean, and the processing of aerosols by clouds. The few in-situ measurements of POCs prior to VOCALS had shown the association of POCs with strong drizzle (Van Zanten and Stevens 2005; Sharon et al. 2006; Comstock et al. 2005, 2007) and very low aerosol concentrations (Petters et al. 2006, Sharon et al. 2006, Wood et al. 2008), consistent with strong precipitation scavenging. Large eddy simulation (LES) studies had suggested that low aerosol concentrations could promote open cell formation (Savic-Jovcic and Stevens 2008).

The present paper describes VOCALS, outlines key scientific activities within the program, and highlights selected achievements. We start in section 2 by describing the major research activities in the program. Section 3 details the importance of coastal circulations. Section 4 highlights issues associated with the ocean heat budget in the SEP. Section 5 describes new research on aerosol-cloud-precipitation interactions. Section 6 discusses how regional and large scale modeling is helping to address VOCALS science questions. Section 7 briefly presents capacity building, before a summary of current activities, science findings and remaining questions.

2. Research Activities

VOCALS research has been organized around two broad sets of hypotheses on coupled ocean-atmosphere-land interactions and aerosol-cloud-precipitation (Wood et al. 2011a). Starting from the hypotheses, a verification strategy was designed to provide the strongest possible synergy between long-term observations and monitoring, intensive field measurements, and modeling. The following subsections highlight activities in these three categories.

a Monitoring: Surface fluxes and drivers over the SEP

Data collected by the WHOI buoy has allowed for the compilation of a surface climatology and air-sea fluxes during the period 2001-2010. At the mooring location and in the annual mean, a remarkably consistent southeasterly wind of ~6 m s^{-1} drives latent heat fluxes exceeding 100 W m^{-2}. Surface precipitation is negligible. The net annual mean surface heat flux is approximately 35 W m^{-2} (positive values indicate ocean warming), with values ranging from 21 W m^{-2} (in 2009) to 60 W m^{-2} (in 2001). Wind speed, air and sea surface temperature and shortwave radiation have marked annual cycles. The annual cycle of net surface heat flux is driven primarily by that in net shortwave radiation because evaporation is approximately constant throughout the year. The upper ocean responds to the surface forcing, with the warmest temperatures and shallowest surface mixed layers occurring in austral fall and the coolest temperatures and deepest mixed layer seen in early spring (Fig. 2). Salinity in the upper ocean also has a seasonal cycle with the shallow summer mixed layer becoming saltier in response to the evaporation. A layer of fresher water (the Eastern South Pacific Intermediate Water; Schneider et al. 2003) lies at a depth of 150 to 250 m below the surface layer.

b The field campaign: VOCALS-REx

VOCALS-REx took place during October and November 2008, when some 150 scientists from 40 institutions in 8 nations gathered in the coast of northern Chile to conduct the field study (Wood et al. 2011a; see Fig. 3). Operations took place in the domain 12-31°S, 69-86°W. In this region, conditions in the atmosphere and upper ocean were near-average with El Niño/Southern Oscillation (ENSO) in its neutral phase. The synoptic forcing was significant during the first half of VOCALS-REx and weak with uninterrupted subsidence during the second half (Rahn and Garreaud 2010b). Sampling concentrated along 20°S from the Chilean coast (70°W) to the

WHOI buoy (85°W). This latitude line was chosen because it transects the heart of the SEP stratocumulus sheet (Klein and Hartmann 1993; George and Wood 2010), exhibits strong longitudinal microphysical contrasts (Bennartz 2007; Wood et al. 2008; George and Wood 2010; Painemal and Zuidema 2010; Bretherton et al. 2010a), crosses a region of frequent open cell formation (Wood et al. 2008), shows evidence of mesoscale ocean eddy activity (e.g. Colbo and Weller 2007; Toniazzo et al. 2009; Colas et al. 2012a,b), and had already been sampled on six previous buoy-tending cruises (e.g., Zuidema et al. 2009; de Szoeke et al., 2010; and references therein). A total of five aircraft (the NSF/NCAR C-130, the DoE G-1, the CIRPAS Twin Otter, and the British FAAM BAe-146 and NERC Dornier 220) from locations on the Chilean coast sampled clouds, aerosols, precipitation, and lower tropospheric structure. The long range of the C-130 and BAe-146 allowed them to operate over the remote ocean over 1000 km offshore. The other aircraft operated primarily in the region to the east of 80°W. A number of different flight patterns were flown (Wood et al. 2011a). Several aircraft flew missions along lines of constant latitude (primarily 20°S) from the coast westward. The Twin Otter flew all its missions in the near coastal region from Iquique to Point Alpha (20°S 72°W, Zheng et al. 2011). Two research vessels (the NOAA Ship Ronald H Brown (RHB) and the Peruvian IMARPE R/V José Olaya) participated in Rex from ports in Chile and Perú. The RHB carried an extensive suite of aerosol instruments, cloud/precipitation remote sensing, rawinsondes, and oceanographic instruments to map the structure of the upper ocean, and in particular locate and investigate mesoscale ocean features (Whelan et al. 2009). The R/V Olaya (Grados et al. 2010; Wood et al. 2011) obtained many profiles and radiosonde launches off the Pisco-San Juan area in southern Perú (13-15°S) and gathered biochemical data and hydroacoustic estimates of fish abundance. In addition, an autonomous underwater vehicle (glider) completed 9 transects perpendicular to the continental

slope obtaining very high resolution information of the ocean currents and other physical properties. A coastal supersite situated in Paposo in northern Chile (25.0°S, 70.3°W) provided a suite of meteorological (surface and upper air; Rutllant et al. 2012) and air chemistry and aerosol measurements (Grados et al. 2010; Chand et al. 2010). Radiosonde launches were also performed at Iquique (20.3°S, 70.1°W) and complemented at Antofagasta (23.5°S) where the Chilean Weather Service maintains a regular station.

c. Model assessment

In preparation for VOCALS, a Preliminary Model Assessment (PreVOCA) of the simulated SEP climate was conducted with an emphasis on the clouds and the MBL. Results from operational forecast, regional, and global climate models were contrasted for the month of October 2006 (Wyant et al. 2010). In general, the models agreed on large-scale dynamics, but performed poorly on cloud properties. The models had great difficulties with the geographic distribution of low cloud cover, with only a few models agreeing well with satellite observations. Most models underestimated MBL depth near the coast at 20°S, and the liquid water path and its diurnal cycle at the WHOI buoy and to the east of it. The near-coastal inversion base height simulated by regional numerical models is about half of the observed values. This problem is common to several models [MM5 (Garreaud and Muñoz 2006), WRF (Rahn and Garreaud 2010a,b), COAMPS (Wang et al. 2011), and MetUM (Abel et al. 2010)] and does not disappear with increasing resolution or by changing turbulence schemes. In contrast, the analysis of a high-resolution WRF simulation concluded that the bias in simulated inversion height may be at least partly caused by increased subsidence aloft due to excessive onshore flow that in reality is strongly blocked by the coastal range (Rahn and Garreaud 2010a,b; Wang et al. 2012). The shallow MBL in the models is usually accompanied by lack of clouds in the near coastal region;

228 but the near-shore surface wind field parallel to the coast is well reproduced in general.

229 A follow-on VOCALS assessment, VOCA, has been completed (see
230 www.atmos.washington.edu/~mwyant/vocals/model/VOCA_Model_Spec.htm). This assessment
231 focuses on four global models including aerosol-cloud processes, and four regional chemical
232 transport models (three of which are versions of WRF-Chem). The period selected is 15 October
233 - 15 November 2008 to use the extensive in-situ observations from VOCALS-REx. Figure 4
234 compares the model simulations with aircraft observations of mean cloud droplet number and
235 MBL boundary-layer sulfate aerosol mass concentrations along 20^0S averaged over the selected
236 period. All models show increasing of sulfate near the Chilean coast due to upwind
237 anthropogenic sources, but its magnitude and effect on the cloud droplet number vary widely
238 between models. The models also showed consistent underestimation of free-tropospheric cloud
239 condensation nucleus concentration over the remote SEP.

240 Another model assessment addressed the simulations of the SEP surface heat budget by
241 CGCMs from the Third Coupled Model Intercomparison Project (CMIP3; de Szoeke et al. 2010).
242 The study concentrated on mean October values along the 20°S line from 75-85°W (between the
243 WHOI and the SHOA buoys). Annual cruises servicing those moorings (section 2a) allowed for
244 reliable estimates of the climatological mean surface heat and radiative fluxes to be calculated,
245 which proved to be in good agreement with three satellite and reanalysis-based surface flux data
246 sets. In October, the mean net solar heating warms the ocean by ~200 W m^{-2}, while longwave
247 radiation and evaporation cool by 25 W m^{-2} and 90 W m^{-2} respectively, and sensible heat flux
248 cools by only 5 W m^{-2} (Fig. 5a). A residual cooling of some 30 W m^{-2} must be provided to a
249 ~50 m thick ocean mixed layer to limit the seasonal SST warming to the observed value of ~0.7°
250 K $month^{-1}$. Some 10 W m^{-2} of solar radiation is estimated to penetrate the 50 m mixed layer

(Zhang et al. 2011). The ocean must provide 20 W m^{-2} cooling, therefore, to balance its heat budget. Observations and models were ranked by their net solar radiation (Fig. 5b). All CGCMs analyzed have at least 30 W m^{-2} too much solar warming. Half of the solar radiation bias is compensated by an increase in longwave cooling (Fig. 5c). These errors are largely explained by weak cloud radiative forcing due to insufficient cloud fraction (Fig. 5d). The lateral ocean cooling, found as a residual, varies among models, but is usually underestimated and can even have the wrong sign.

3. The coastal circulation

a. Wind and MBL structure

The data collected by the R/V Olaya reveal a great deal of alongshore variability of the near surface wind field with local maxima just to the north of major headlands and minima father downstream (e.g., Rahn et al. 2011), imprinting the upper ocean of these regions. The seasonal mean height of the MBL inversion, on the other hand, is remarkably uniform at about 1000 m above sea level along the coast for more than 700 km between Arica (18°S) and Paposo (25°S) although SST cools gradually from north to south (Rahn and Garreaud 2010a). This height of the MBL inversion coincides with the coastal range elevation, which is quite uniform over this range of latitudes. The inversion height remains about constant at least up to 200 km offshore. In the near coastal zone the MBL tends to be cloud capped and well mixed, with the maximum inversion strength at 100-200 km off the coast.

Synoptic-scale disturbances (upper-level troughs and cutoff lows) propagating from midlatitudes into the subtropics can intermittently strengthen subsidence and deepening of the coastal MBL up to 1500 m (Rutllant et al. 2012) in northern Chile and also offshore (Rahn and Garreaud 2010b; Toniazzo et al. 2011). These synoptic conditions are associated with more

polluted but also thinner coastal clouds, with the thin clouds limiting the overall radiative impact of the aerosols trapped in the marine boundary layer (Painemal and Zuidema, 2010; George and Wood, 2010; Twohy et al. 2012). Offshore, the southerly winds above the marine boundary layers are weakened, increasing the offshore lower tropospheric stability and offshore cloud cover (Painemal and Zuidema, 2010; Wyant et al., 2010).

b. Diurnal cycle of cloud and precipitation over the SEP

Ship observations capture diurnal cycles of cloud fraction, liquid water path, thermodynamic decoupling between the surface and cloud, and precipitation (de Szoeke et al. 2012; Burleyson et al. 2013). The strongest diurnal cycles are related to the diurnal cycle of MBL depth. Cloud fraction, cloud thickness, liquid water path, and precipitation increase at night when solar warming of the cloud top ceases, but longwave cooling continues. The displacement between cloud base and the lifting condensation level (LCL) of air at the surface is a thermodynamic proxy for turbulent decoupling and suppressed mixing between the surface layer and the cloud. Cloud base-LCL displacement grows during the day, but the cloud rapidly recouples to the surface layer at night. Cloud fraction is reduced during the day as the cloud rises and entrains dry air, while moisture flux from the surface layer to the cloud is suppressed through the stable subcloud boundary layer. Precipitation has a diurnal maximum in the early morning. West of 80°W, the precipitation begins to decrease before the sun rises, raising the possibility that the precipitation limits itself. Perhaps sub-cloud evaporative cooling of rain establishes a local stable layer sufficient to reduce the precipitation. Decoupling and precipitation are stronger in the mean west of 80°W, and have stronger diurnal cycles west of 80°W than east of 80°W.

The diurnal cycle of cloud properties over the SEP shows significant semidiurnal contribution with especially strong amplitude close to the Peruvian and Chilean coastline in October but also reaching locations over 1500 km offshore (Garreaud and Muñoz 2004; O'Dell et al. 2008; Wood et al. 2009; Zuidema et al. 2009; Rahn and Garreaud, 2010a, de Szoeke et al. 2012). These behavior highlights that factors other than solar radiation are important for the diurnal cycle of clouds and precipitation over the SEP. Toniazzo et al. (2011) on the basis of simulations with the Weather and Research Forecast (WRF) regional model, showed that the diurnal variability over the SEP is the result of superposition of a locally solar-induced diurnal cycle and remotely forced, propagating signals forced by the thermally direct circulations over the west- and south-west facing slopes of the Andes. A deep wave with a 24-hour period is generated over the Peruvian orography, and moves southwestward, and a weaker, shallower wave with a significant semi-diurnal component propagates westward from the Chilean orography. These waves are primarily confined to the lower troposphere, and their impact on the inversion at the top of the MBL is substantial within ~5 degrees from the coast. As they move towards the open ocean, the remotely generate down and upwelling waves can be either in phase, out of phase or phase lagged with respect to variation locally forced by solar radiation. Since the waves gradually disperse or dissipate while propagating, a clear semidiurnal signal appears only near coastal regions.

c. Ocean upwelling and mesoscale eddies

The coastal ocean along the Chilean and Peruvian coasts is characterized by upwelling that drives ocean biological productivity and is a key source region for mesoscale ocean eddies (Grados et al. 2010; Garreaud et al. 2011). The surface alongshore ocean circulation in the northern boundary of the most intense upwelling cell of Peru - the Pisco-San Juan upwelling -

was studied at a weekly frequency during VOCALS-REx with a Slocum glider. The glider measured temperature, salinity, fluorescence and oxygen at a high spatial resolution (~ 2 km) along a ~100 km cross-shore section near 14°S. Using the drift of the glider between two dives and T-S profiles for thermal wind allowed to compute the absolute geostrophic current over the 200-m deep surface layer. The offshore surface equatorward jet and nearshore subsurface poleward nundercurrent display a high variability at weekly time scales (Fig. 6), generating variable horizontal and vertical shear for instabilities. These measurements also provided invaluable insights on the submesoscale upwelling dynamics responsible for the subsurface cross-isopycnal salinity intrusions (Pietri et al. 2012).

Chaigneau et al. (2011) used Argo float profiles and satellite altimetry data to estimate the mean vertical structure of mesoscale eddies in the Peru-Chile Current System. Their estimates are consistent with the core of cyclonic eddies being centered at ~150 m depth, and that of the anticyclonic eddies below the thermocline at ~400 m depth. They also argue that each cyclonic and anticyclonic eddy yields to a heat and salt transport anomaly of $\pm 1\text{–}3 \times 10^{11}$ W and $\pm 3\text{–}8 \times 10^{3}$ kg s^{-1}, respectively. These eddies propagate westward across the area of VOCALS region, contribute the dominant signal in oceanic velocities at the WHOI buoy, and influence biology (Chelton et al. 2011).

4. The ocean heat budget

Unveiling the mechanisms for cooling of the ocean column under the stratocumulus has been one of VOCALS main concerns. As indicated in the Introduction, Colbo and Weller (2007) suggested that the mean ocean circulation, including geostrophic and Ekman transport, may be insufficient to balance the warming of the ocean column by surface heat fluxes. In a first attempt to shed light on this issue, Toniazzo et al (2009) examined heat transport by ocean eddies away

342 from the coast by using HiGEM, a CGCM with relatively high resolution in the global ocean
343 ($1/3^{o}\times1/3^{o}$). In the SEP, HiGEM simulates significant contributions to the long-term mean heat
344 budget of the water column from heat advection by ocean transients with length scales of 200-
345 450 km, and time scales between 4 month and one year. At least part of the heat advection is due
346 to transients associated with an intrusion of fresh water from higher latitudes along the east-
347 Pacific coast. This contribution is highly variable both in space and time, and its magnitude at the
348 location of the WHOI buoy is consistent with the estimate by Colbo and Weller (2007). The
349 contribution of eddies further out at 85°W is unclear and can be of either sign in the ocean
350 interior (see also Zheng et al. 2010). Holte et al (2012), based on the analysis of observational
351 data from the region found that the contribution of the eddy heat flux to the surface layer is, on
352 average, small over the SEP.
353 The heat budget problem was addressed by Colas et al. (2012a,b) using a regional, eddy-
354 resolving ocean model (7.5km×7.5km). According to the results, an important component of the
355 lateral heat flux is by mesoscale eddies in the pycnocline, associated with an adiabatic down-
356 gradient release of available potential energy and an eddy-induced Lagrangian overturning
357 circulation largely in the opposite sense to the Eulerian mean upwelling circulation. The
358 offshore vertical heat balance is then completed by a shallow submesoscale restratification
359 buoyancy and heat flux in a second cell of eddy-induced circulation within the surface boundary
360 layer and upper pycnocline, where it is significantly diabatic (cross-isentrope) in combination
361 with (and opposition to) diabatic downward heat flux from the boundary layer turbulent mixing.
362 In both these circulations the eddy heat flux is primarily shoreward and upward. Colas et al
363 (2012a) also found that cyclonic vortices tend to dominate the surface field, whereas anticyclonic
364 vortices dominate the subsurface. The Undercurrent sheds coherent subsurface anticyclones with

365 warm and salty cores, in agreement with the observational results of Chaigneau et al. (2011; see
366 subsection 3c).
367 Some controversy remains in the understanding about the vertical heat fluxes in the upper
368 ocean and their role on the SST.. In the results of Colas et al. (2009), in the surface layer the
369 divergence of the heat flux by eddies corresponds to heating and that by the mean flow
370 corresponds to cooling. The integrated heat flux divergence in parts of the ocean column must
371 be balanced through vertical heat transports by turbulence, sub-mesoscale eddy, and possibly
372 other effects yet to be determined. A better understanding of these effects may require long time
373 series of upper ocean measurements.

374 ## 5. Aerosol-cloud-precipitation interactions

375 One of VOCALS central goals is the better understanding of interactions between clouds,
376 aerosols and precipitation. VOCALS-REx observations were collected to address factors
377 controlling precipitation and POC formation, how anthropogenic pollution is transported to the
378 MBL and affects cloud microphysics, and the role played by precipitation in removing aerosol
379 particles from the atmosphere. This section highlights a few of the new findings.

380 *a. Structure of a stratocumulus region: clouds, MBL structure and aerosols along 20°S.*

381 The 20°S synthesis constructed using data from the five aircraft and the RHB
382 participating in VOCALS-REx (see Fig. 7) provides insight into the processes controlling
383 stratocumulus variability on the regional and synoptic scales (Bretherton et al. 2010a; Allen et al.
384 2011), and is being used to test climate models (section 6c). Cloud top, situated immediately
385 beneath a strong inversion, rises sharply from the coast offshore (Fig 7a). (Here data from the
386 seven research cruises in the VOCALS region were used to build a climatology). A concomitant
387 rise in cloud base means that ~50% of the clouds sampled were considered decoupled from the

surface (Jones et al. 2011). Low cloud cover remains above 80% over the entire transect, but the amount of condensate almost doubles offshore (Fig 7b) because cloud thickness increases. This helps to drive stronger precipitation offshore (Fig 7c). Reduced cloud droplet concentrations due to lower aerosol concentrations offshore (Fig 7d) also likely increase the offshore precipitation gradient (Terai et al. 2012), but cloud resolving modeling suggests that cloud top height may have a stronger control on precipitation than aerosols (Mechem et al. 2012). Along 20°S the submicron aerosol is dominated by sulfates (Fig. 7e), with organic species accounting for less than 30% of the aerosol mass (Hawkins et al. 2010; Allen et al. 2011) and less than this in the more unpolluted airmasses over the remote ocean (Shank et al. 2012). The increased sulfate loading near the coast is driven primarily by anthropogenic pollutants from smelters and the Santiago megacity (Yang et al. 2011, Saide et al. 2012a) rather than by enhanced DMS near the coast. On the other hand, DMS is the primary source in the sulfate mass budget over the remote ocean west of 80°W where VOCALS observations showed that DMS sea-air fluxes and atmospheric concentrations are greater than those near the coast (Yang et al. 2009).

b. Pockets of open cells: extreme coupling between clouds, aerosols and precipitation

Flights were dedicated during VOCAL-REx to study the spatial transition between POCs and overcast stratocumulus, and the relative influence of aerosols and meteorology on POC formation. The RHB also sampled POCs (Waliser et al. 2012) during REx. All of the POCs sampled during VOCALS showed strong microphysical gradients across the boundaries (Painter et al. 2012) and ultraclean layers (Wood et al. 2011b) near the MBL top. It appears, therefore, that the microphysical contrasts between POCs and the surrounding cloud is a robust feature. At the very low droplet concentrations that typify POCs, model studies show a strong sensitivity of cloud cover to cloud droplet concentration (Ackerman et al. 2003; Wang and Feingold 2009a,b;

411 Wang et al. 2010; Berner et al. 2011). Thus it seems reasonable to posit that strong depletion of
412 aerosols is a fundamental component of a POC. That said, studies also suggest that relatively
413 small meteorological differences (Wang et al. 2010) and gravity waves (Allen et al. 2012) can
414 also drive POC formation. Precipitation in POCs is locally heavier but less frequent than that in
415 the surrounding cloud (Comstock et al. 2005; Wood et al 2011a; Painter et al. 2012), is central
416 for maintaining the cold pools that drive the open cell dynamics (Feingold et al. 2010) and is the
417 main cause of aerosol depletion in the POC.

418 Thus POCs constitute a remarkably extreme case of aerosol-cloud-precipitation coupling
419 (see Fig. 8). POCs are also strongly coupled to the surrounding stratocumulus clouds through
420 secondary circulations atop the MBL that are important for maintaining the height of the MBL
421 despite reduced entrainment in the POC (Bretherton et al. 2010b; Berner et al. 2011). Since many
422 stratocumulus clouds produce significant precipitation globally (Leon et al. 2009), it is
423 reasonable to posit that this close aerosol-cloud-precipitation coupling seen in extreme form in
424 POCs is also important for controlling marine cloud systems more generally (Wood et al. 2012).

425 VOCALS is also shedding light on how an aerosol population is maintained within POCs
426 against losses to precipitation. Recent modeling work (Kazil et al. 2011) indicates that surface
427 sea-salt, new particle formation from the oxidation of DMS, and entrainment of particles from
428 the free troposphere may all contribute significantly to POC aerosol maintenance. Accumulation
429 mode aerosol concentrations near the surface within POCs are remarkably similar from case to
430 case (Painter et al. 2012) despite differences in the sources. This hints at possible self-regulating
431 aerosol populations within POCs that are yet to be fully understood.

c. Aerosol impacts on clouds: the importance of the free-troposphere

It is becoming clear from measurements made during VOCALS-Rex, that because the region sampled is typified by large-scale subsidence,there is almost always a flux of free-troposphere (FT) aerosol into the MBL. For a nominal inversion at ~1 km altitude and mean cloud top entrainment rates of 0.3-0.6 cm s^{-1} (Wood and Bretherton 2004; Caldwell et al. 2005), this implies an entrainment of about 250-500 m day^{-1} of FT air, which would rapidly dilute MBL concentrations of cloud concentration nuclei (CCN) if the entrained air were particle-free. However, FT aerosol over the VOCALS region varies markedly in total aerosol number and in sizes effective as CCN in the MBL such that entrainment and mixing of FT air may act to raise or lower MBL concentrations. In addition to any aerosol flux, the entrainment of FT air can also modify MBL thermodynamic and moisture properties can impact MBL boundary layer clouds in complex ways (Ackerman et al.2004, Wood, 2012).

Characteristic patchiness in carbon monoxide (CO, a gas phase combustion tracer) is shown in Fig. 9 over a distance of ~1000 km along 20°S for a C-130 aircraft flight RF3 on 21 Oct 2008. CO is generally higher aloft and present in patches or "rivers" a few tens of meters to a few hundred meters thick and tens to hundreds of kilometers in extent. West of 78°W the FT winds above the inversion are predominantly southerly but are northerly to the east (Toniazzo et al., 2011). We focus here on the FT west of 78°W as more representative of the remote SEP. The underlying MBL air is typically advected from the pristine South Pacific and on this day a layer of enhanced CO and combustion aerosol from the western Pacific lies just above the inversion and MBL clouds. On other flights, similar layers of combustion outflow from South America to the SE were more common. The size distributions present in air enhanced in CO tend to have higher concentrations of aerosol present in sizes greater than 50nm (N_{gt50}) than in

cleaner FT air (Fig. 9b). In the MBL, a minimum in the number size-distribution is centered close to 75 nm diameter (Tomlinson et al. 2007), but is broad enough to include sizes down to 50nm, indicating most MBL aerosol larger than this acted as CCN in the MBL clouds (Hoppel et al., 1986). Therefore entrainment of air with high CO into the MBL introduces more N_{gt50} (CCN) than does entrainment of the cleaner FT air more common south of the VOCALS region. N_{gt50} for above-cloud legs west of 78°W (Fig. 9c) also increases with black carbon aerosol mass (a combustion aerosol tracer seen to track with CO) from values between about 100 ± 50 cm^{-3} to double that number for elevated CO. Because scavenging of MBL aerosol by drizzle is a strong sink for MBL aerosol west of 78W (Wood et al. 2012), entrainment of FT particles with sizes larger than 50 nm can help buffer MBL CCN concentrations against depletion.

Clean MBL and FT air advected into the VOCALS region have the lowest concentrations of CO (<60 ppbv) along 20°S. Because the highest CO values found over the SEP occur in the FT, entrainment of this air into the MBL during boundary layer advection toward the 20°S latitude line can increase MBL CO concentrations to values exceeding those entering the SEP from the pristine southern Pacific. For example, entrainment at 0.6 cm s^{-1} into a 1000m MBL over about 2 days would yield a 50:50 mix of clean MBL air (low CO at <60 ppbv) with FT air (most frequent CO about 70 ppbv west of 78W) and would raise MBL mixed values to about 64 ppbv. Because 64 ppbv is the most frequent value in the MBL along 20S west of 78W, this suggests most of this air is influenced by entrainment of CO from the FT . Since POCs typically have CO <60 ppbv they appear to have formed only in MBL air least influenced by entrainment of combustion aerosol. Hence, improved understanding of the FT aerosol and factors that modulate its entrainment into the MBL will be essential to understanding the MBL CCN budget and associated cloud properties.

6. Modeling

a. Regional and global dynamical models

Several studies have used WRF in support of VOCALS, and the analysis of results has raised some questions on the model's representation of various physical processes. Andrejczuk et al. (2012), for example, reported that WRF captures the formation of mesoscale cloud-free regions that resemble POC. However, the mechanisms at work seem more dominated by dynamical processes associated with variations in subsidence, while those in LES models seem to be more dominated by physical processes associated with drizzle. Toniazzo et al. (2012) reported a clear sensitivity of their WRF simulations to the choice of vertical grid, limiting the possibility of solid quantitative statements on the amplitudes and phases of the diurnal and semidiurnal components across the domain.

The association based on an analysis of in-situ data has been widely used in diagnostic studies as well as in parameterizations. Sun et al. (2011) showed that the relationship between marine low cloud cover variability in the Southeast Pacific and lower-tropospheric stability (LTS) proposed by Klein and Hartmann (1993) is strongly modulated by the seasonal cycle and by ENSO. Sun et al. (2010) demonstrated that errors in stratocumulus cover over the SEP in the NCEP Global Forecast System (GFS) model can be alleviated by limiting the strength of shallow convective mixing across the inversion with algorithms based on the implementation of direct and physically-based improvements in the model parameterizations. Abel et al. (2010) showed that in the remote maritime region the Met Office forecast model provides a good representation of synoptically induced variability in both cloud cover and MBL depth. The simulation of the diurnal cycle phase is also successful, but the coastal clearing of cloud in certain days is missed. Drizzle is likely to be too strong, and POCS are not captured (section 4b).

b) Regional modeling with integrated chemistry and aerosols

The WRF-Chem model couples dynamical, chemical, aerosol, and cloud processes and can be run at the regional scale (Grell et al. 2005, Fast et al. 2006). Studies with high resolution WRF-Chem and other LES are demonstrating that coupled cloud-aerosol-radiation processes are important for the successful simulation of SEP stratocumulus (Wang et al. 2010; Kazil et al. 2011). Yang et al. (2010) used WRF/Chem to show that inclusion of full aerosol-cloud couplings leads to significant improvements in many key features of the simulated stratocumulus clouds (e.g., cloud top effective radius, cloud water path, and cloud optical thickness. The model is able to capture daily/synoptic scale variations of aerosol and cloud properties. Saide et al. (2012a) argued that WRF-Chem simulates marine cloud-aerosol interactions at a level sufficient for applications in forecasting weather and air quality and studying aerosol climate forcing, and may do so with the reliability required for policy analysis. Both studies highlight the importance of reproducing gradients of aerosol and cloud droplet concentrations that typify the SEP region. Saide et al. (2012b), on the basis of the remarkably robust correspondence of satellite-derived cloud droplet concentrations to in-situ VOCALS data (Painemal and Zuidema 2011; King et al. 2012; Min et al. 2012), are assimilating satellite-observed cloud droplet concentration into WRF-Chem to better constrain aerosol properties below the clouds. WRF-Chem has also been used to provide the first model based regional quantification over the SEP of the aerosol indirect effects on climate (Yang et al. 2012). WRF-Chem is also being used to describe a free-tropospheric transport pathway for aerosol transport to the remote SEP (George et al. 2013).

c. Model development

Process-level understanding developed from VOCALS observations and large eddy modeling is being used to improve physical parameterizations in global models. It can be said

that VOCALS has contributed to accelerate the improvement in the representation of MBL clouds in major modeling centers around the world. For example, in-situ cloud and drizzle observations from REx have been used to refine the microphysical parameterization in the Met Office Unified Model (Boutle and Abel 2012). One of the VOCALS case studies is being used in the WMO Cloud Modeling program (http://slayoo.github.com/icmw2012-case1/) to examine how different models represent the processing of aerosols by clouds.

Observations from REx are a central component of two NSF/NOAA sponsored Climate Process Teams (CPTs) that began in 2010. The CPTs bring together observational scientists, process modelers, and model developers in order to accelerate the rate at which field observational knowledge is translated into improved large-scale models. Both CPTs focus upon cloud processes. One CPT, led by Vincent Larson at the University of Wisconsin-Milwaukee, focuses upon improved representation of subgrid variability in the NCAR Community Atmospheric Model (CAM) and the GFDL Atmospheric Model based on the incorporation of a higher order closure parameterization that accounts for the covariability of moisture, temperature and vertical velocity. REx observations are being used in a number of different ways to evaluate the parameterization and the models into which it is being incorporated (Yamaguchi et al. 2012). A second CPT, led by Joao Teixeira at the NASA/Jet Propulsion Laboratory, aims to improve the representation of the stratocumulus-to-cumulus transition in the CAM and the NCEP Global Forecast System models.

7. Capacity building

Many students participated in VOCALS-REx alongside seasoned scientists, both out at sea and in the air. This is leading to numerous student-led publications (see, e.g., Berner et al. 2011; George and Wood 2010; Hawkins et al. 2010; Jones et al. 2011; Painemal et al. 2010,

2011; Shank et al. 2011; Terai et al. 2012; Zheng et al. 2011) and PhD theses. Students served as flight scientists on many aircraft missions and helped in mission planning. VOCALS participants also reached out to both English and Spanish-speaking K-12 classrooms through the 'Windows to the Universe' (W2U) project led by R. Johnson at NCAR. Within W2U, VOCALS scientists submitted dozens of "Postcards from the Field" describing their field research experiences to inspire the next generation of scientists.

VOCALS also provided learning opportunities to K-12 students and teachers. NOAA's Teacher at Sea Program permitted one teacher to participate in VOCALS-REx on the RHB cruise

8. Current activities, summary of findings, and remaining questions

At the present time, the VOCALS community is engaged in detailed analyses of the datasets collected by REx, as well as other information for the period of the field campaign. The data are being used for support of research leading to parameterization revision for model improvement.

VOCALS set up very ambitious goals, and progress has been achieved in several fronts.

- A unique dataset has been produced by VOCALS-REx and is available to the research community as integrated datasets and through the VOCALS Data Archive (http://www.eol.ucar.edu/projects/vocals/). The WHOI buoy data are currently not used for model assimilation and so represent a unique independent resource for model validation.
- The VOCA model assessment suggests that the REx data will continue to provide important constraints on aerosol-chemistry-cloud interactions in the next generation of climate and chemical transport models. In particular, the sampling across strong microphysical gradients along 20°S is providing a unique dataset to confront models. The gradients are caused by

pollution aerosol and by a longitudinal gradient in precipitation. Some of the pollution aerosol is transported offshore in the free troposphere and then entrained into the clouds.

- The air-sea exchanges across the region at 20°S, from 85°W to 75°W, are well described. It has been firmly established that mean advection and eddy advection both contribute importantly to the heat budget of the ocean column in the SEP, though to varying degrees dependent upon the offshore distance and the difference between Peru and Chile.
- The existence of a daytime upsidence wave initiated by Andean slope heating that propagates over 1500 km offshore over the southeastern Pacific stratocumulus region has been confirmed. The wave impacts clouds by strengthening the diurnal cycle, which reduces daytime cloud albedo and increases nocturnal precipitation.
- Strong depletion of aerosols driven by precipitation losses appears to be a fundamental component of POCs. Precipitation in takes on a fundamentally distinct character from that in the surrounding cloud, with cold pools driving a reorganization of the mesoscale structure and dynamics. POCs can be triggered by reduced aerosol concentrations but also by modest moisture and temperature perturbations and by gravity waves.
- Slow aerosol replenishment in the ultra-clean POC environment permits the maintenance of open cells. The aerosol sources are a combination of mechanical surface production, entrainment of aerosol from above the inversion, and nucleation of new particles in the cloud-scavenged ultra-clean layer below the inversion.
- Maintenance of open-cells is also dependent on the self-organization within the system. The sub-cloud evaporation of precipitation drives cold pools, and the interaction between these cold pools helps regenerate clouds.

- The first aerosol indirect effect has been observationally quantified over the SEP, with cloud thinning of the more polluted coastal clouds mitigating the overall radiative impact. The effects were also quantified in the region using a regional model.

However, several issues and questions remain:

- Some controversy remains in the understanding of the vertical heat transports by turbulence, sub-mesoscale eddies, and possibly other processes, and on the role of such processes in determining the SST in the SEP.
- The relative contributions of surface, entrainment, and nucleation aerosol sources to the aerosol budget in the remote MBL remains poorly understood.
- The frequency and climatic importance of POCs remains poorly-characterized. A full assessment of all triggering mechanisms for POC formation given realistic aerosols and meteorology has not yet been conducted. The ability of anthropogenic pollutants to hinder the formation of POCs is also not yet known, with the implied significant increase in albedo important for geoengineering (Rosenfeld et al. 2006).

The impetus on the research on VOCALS issues in the SEP continues unabated. One year after VOCALS-REx - in late spring 2009 - the Chilean Upwelling Experiment (CUpEx) in the near-shore region of 30°S focused on the ocean-atmosphere interaction in a major upwelling center off northern Chile (Garreaud et al. 2011). CUpEx included two radiosonde stations, several ground stations, buoys, and marine radars. This experiment has confirmed finding of VOCALS-Rex in the coastal SEP and provided additional detailed information on coastal processes.

VOCALS is also motivating research in other major upwelling regions. Coupled GCMs suffer from common biases in the eastern Atlantic Ocean that resemble those in the Pacific. Observational research has an active history in the equatorial Atlantic also, e.g., the PIRATA

buoy array and research cruises, aircraft campaigns, and the recent AMMA program. VOCALS and Atlantic researchers are planning joint activities under the U.S. CLIVAR Working Group on Eastern Tropical Ocean Synthesis (http://www.usclivar.org/working-groups/etos) with the ultimate goal of further reducing the SST biases of CGCMs using targeted process studies and model assessments.

Acknowledgements.

The authors are grateful to Casey D. Burleyson, Matt Wilbanks, Matt Wyant, Vincent Echevin, and Alice Pietri for their contributions to the manuscript. Many people have contributed to VOCALS; we will attempt to recognize at least some of the key groups. The cooperation of the Chilean Navy Hydrographic and Oceanographic Service (SHOA) in work on the mooring at 75°W is gratefully acknowledged. VOCALS is grateful to the support staff, crew and scientists of its six aircraft platforms (the NSF/NCAR C-130, the UK FAAM BAe-146, the DoE G-1, the CIRPAS Twin Otter, the UK NERC Dornier 228, and, in the 2010 CUpEx phase, the Chilean King Air), two ships (the NOAA Ronald H Brown, and the Peruvian IMARPE José Olaya), and land stations at Iquique and Paposo. José Meitin and colleagues at the NCAR Earth Observing Laboratory coordinated and executing field logistics and data archive support for VOCALS Rex. Mike Patterson at NOAA and currently at US CLIVAR championed VOCALS during its development stages. W. Robinson at NSF, J. Huang at NOAA, and Howard Cattle and David Legler at CLIVAR's International and US CLIVAR's Project Office coordinated the U. S. agency support.

References

Abel, S. J., Walters, D. N., and Allen, G., 2010: Evaluation of stratocumulus cloud prediction in the Met Office forecast model during VOCALS-REx, *Atmos. Chem. Phys.*, **10**, 10541-10559.

Ackerman, A. S., O. B. Toon, D. E. Stevens, and J. A. Coakley Jr., 2003: Enhancement of cloud cover and suppression ofnocturnal drizzle in stratocumulus polluted by haze, Geophys. Res. Lett., 30(7), 1381, doi:10.1029/2002GL016634.

Ackerman, A. S., M. P. Kirkpatrick, D. E. Stevens, and O. B. Toon, 2004: The impact of humidity above stratiform clouds on indirect aerosol climate forcing. *Nature*, **432**, 1014-1017, doi:10.1038/nature03174.

Allen, G., H. Coe, A. Clarke, C. Bretherton, R. Wood, S. J. Abel, P. Barrett, P. Brown, R. George, S. Freitag, C. McNaughton, S. Howell, L. Shank, V. Kapustin, V. Brekhovskikh, L. Kleinman, Y. –N. Lee, S. Springston, T. Toniazzo, R. Krejci, J. Fochesatto, G. Shaw, P. Krecl, B. Brooks, G. McMeeking, K. N. Bower, P. I. Williams, J. Crosier, I. Crawford, P. Connolly, J. D. Allan, D. Covert, A. R. Bandy, L. M. Russell, J. Trembath, M. Bart, J. B. McQuaid, J. Wang, and D. Chand, 2011: South East Pacific atmospheric composition and variability sampled along 20° S during VOCALS-REx, *Atmos. Chem. Phys*., **11**, 5237-5262, doi:10.5194/acp-11-5237-2011.

Allen, G., Vaughan, G., Toniazzo, T., Coe, H., Connolly, P., Yuter, S. E., Burleyson, C. D., Minnis, P. and Ayers, J. K. (2012), Gravity-wave-induced perturbations in marine stratocumulus. Q.J.R. Meteorol. Soc.. doi: 10.1002/qj.1952

Andrejczuk, M., W. W. Grabowski, A. Gadian, and R. Burton, 2012: Limited-area modelling of stratocumulus over South-Eastern Pacific. *Atmos. Chem. Phys.*, **12**, 3511-3526.

657 Bennartz, R., 2007: Global assessment of marine boundary layer cloud droplet number
658 concentration from satellite. J. Geophys. Res., 112, D02201, doi:10.1029/2006JD007547
659 Berner, A. H., C. S. Bretherton, and R. Wood, 2011: Large-eddy simulation of mesoscale
660 dynamics and entrainment around a pocket of open cells observed in VOCALS-REx *Chem.*
661 *Phys.*, **11**, 10525-10540.
662 Boutle, I. A. and Abel, S. J., 2012: Microphysical controls on the stratocumulus topped
663 boundary-layer structure during VOCALS-REx, *Atmos. Chem. Phys*., 12, 2849-2863,
664 doi:10.5194/acp-12-2849-2012.
665 Bony, S., and J.-L. Dufresne, 2005: Marine boundary layer clouds at the heart of tropical cloud
666 feedback uncertainties in climate models, *Geophys. Res. Lett.*, 32, L20806,
667 doi:10.1029/2005GL023851.
668 Bretherton, C. S., T. Uttal, C. W. Fairall, S. E. Yuter, R. A. Weller, D. Baumgardner, K.
669 Comstock, and R. Wood, 2004: The EPIC 2001 Stratocumulus Study. *Bull. Amer. Met. Soc.*,
670 85, 967-977.
671 Bretherton, C. S., R. Wood, R. C. George, D. Leon, G. Allen, and X. Zheng, 2010a: Southeast
672 Pacific stratocumulus clouds, precipitation and boundary layer structure sampled along 20°S
673 during VOCALS-REx. *Atmos. Chem. Phys*, **10**, 10639-10654.
674 Bretherton, C., J. Uchida, and P. N. Blossey, 2010b: Slow manifolds and multiple equilibria in
675 stratocumulus-capped boundary layers. Submitted to *J. Adv. Model. Earth Syst.*, http://adv-
676 model-earth-syst.org/index.php/JAMES/article/view/52.
677 Burleyson, C. D., S. P. de Szoeke, S. E. Yuter, M. Wilbanks and W. A. Brewer, 2013:
678 Observations of the Diurnal Cycle of Southeast Pacific Marine Stratocumulus Clouds and
679 Precipitation. *J. Atmos. Sci*, submitted 2012 December 14.

680 Caldwell, P., C. S. Bretherton, and R. Wood, 2005: Mixed layer budget analysis of stratocumulus
681 dynamics during EPIC. *J. Atmos. Sci.,* **62**, 3775-3791.

682 Colbo, K. and R. Weller, 2009: The accuracy of the IMET sensor package in the subtropics. *J.*
683 *Atmos. Oc. Tech..,* **26**, 1867–1890.

684 Comstock, K. K., R. Wood, S. E. Yuter, and C. S. Bretherton, 2004: Reflectivity and rain rate in
685 and below drizzling stratocumulus. *Quart. J. Roy. Meteor. Soc*., **128**, 2891-2918.

686 Comstock, K. K., C. S. Bretherton, and S. E. Yuter, 2005: Mesoscale variability and drizzle in
687 southeast Pacific stratocumulus. *J. Atmos. Sci.*, **62**, 3792-3807.

688 Comstock, K. K., S. E. Yuter, R. Wood, and C. S. Bretherton, 2007: The three-dimensional
689 structure and kinematics of drizzling stratocumulus. *Mon. Wea. Rev*., **135**, 3767-3784.

690 Chaigneau, A., M. Le Texier, G. Eldin, C. Grados, and O. Pizarro, 2011: Vertical structure of
691 mesoscale eddies in the eastern South Pacific ocean: a composite analysis from altimetry
692 and Argo profiling floats. J. Geophys. Res., 116, C11025, doi:10.1029/2011JC007134.

693 Chand, D., D. A. Hegg, R. Wood, G. E. Shaw, D. Wallace, and D. S. Covert, 2010: Source
694 attribution of climatically important aerosol properties measured at Paposo (Chile) during
695 VOCALS, *Atmos. Chem. Phys.*, **10**, 10789-10801, doi:10.5194/acp-10-10789-2010.

696 Colas, F., X. Capet, J.C. McWilliams, and Z. Li, 2012a: Mesoscale eddy buoyancy flux and
697 eddy-induced circulation in eastern-boundary upwelling systems. *J. Phys. Ocean*., in press.

698 Colas, F., J. C. McWilliams, X. Capet, and K. Jaison, 2012b: Heat balance and eddies in the
699 Peru-Chile current system. *Clim. Dyn.*, **39**, 509-529, 10.1007/s00382-011-1170-6.

700 Colbo, K. and R. Weller, 2007: The variability and heat budget of the upper ocean under the
701 Chile-Peru stratus. *J. Marine. Res.*, **65**, 607–637.

Chelton, D. B., P. Gaube. M. G. Schlax, J. J. Early, and R. M. Samelson, 2011: The influence of mesoscale eddies on near-surface oceanic chlorophyll. *Science,* **334** no. 6054, 328-332 DOI: 10.1126/science.1208897

Davey, M. K., M. Huddleston, K. R. Sperber, P. Braconnot, F. Bryan, D. Chen, R. A. Colman, C. Cooper, U. Cubasch, P. Delecluse, D. DeWitt, L. Fairhead, G. Flato, C. Gordon, T. Hogan, M. Ji, M. Kimoto, A. Kitoh, T. R. Knutson, M. Latif, H. Le Treut, T. Li, S. Manabe, C. R. Mechoso, G. A. Meehl, S. B. Power, E. Roeckner, L. Terray, A. Vintzileos, R. Voss, B. Wang, W. M. Washington, I. Yoshikawa, J.-Y. Yu, S. Yukimoto and S. E. Zebiak, 2001: STOIC: a study of coupled model climatology and variability in tropical ocean regions. *Climate Dynamics*, **18**, 403-420.

de Szoeke, S. P., C. W. Fairall, D. E. Wolfe, L. Bariteau, and P. Zuidema, 2010: Surface Flux Observations on the Southeastern Tropical Pacific Ocean and Attribution of SST Errors in Coupled Ocean-Atmosphere Models. *J. Climate*, **23**, 4152-4174, 10.1175/2010jcli3411.1.

de Szoeke, S. P., and S. –P. Xie, 2008: The Tropical Eastern Pacific Seasonal Cycle: Assessment of Errors and Mechanisms in IPCC AR4 Coupled Ocean–Atmosphere General Circulation Models. *J. Climate*, **21**, 2573-2590.

de Szoeke, S. P, S. Yuter, D. Mechem, C. Fairall, C. Burleyson, and P. Zuidema, 2012: Observations of stratocumulus clouds and their effect on the eastern Pacific surface heat budget along 20°S. *J. Climate*, 8542-8567.

Fast, J. D., Gustafson, W. I., Easter, R. C., Zaveri, R. A., Barnard, J. C., Chapman, E. G., Grell, G. A., and Peckham, S. E.: Evolution of ozone, particulates, and aerosol direct radiative forcing in the vicinity of Houston using a fully coupled meteorology-chemistry-aerosol model, J. Geophys. Res-Atmos., 111, D21305, doi:10.1029/2005jd006721, 2006.

725 Feingold, G., I. Koren, H. Wang, H. Xue, and W. A. Brewer, 2010.: Precipitation generated
726 oscillations in open cellular cloud fields. *Nature*, **466**, 849–852.
727 Garreaud, R. D., J. A. Rutllant, R.C. Muñoz, D. A. Rahn, M. Ramos, and D. Figueroa, 2011:
728 VOCALS-CUpEx: the Chilean Upwelling Experiment. *Atmos. Chem. Phys*., **11**, 2015-2029,
729 doi:10.5194/acp-11-2015-2011.
730 Garreaud, R. D., and R. Muñoz, 2004: The diurnal cycle in circulation and cloudiness over the
731 subtropical southeast Pacific: A modeling study. J. *Climate*, **17**. 1699-1710.
732 Garreaud, R. D., J. A. Rutllant, R. C. Muñoz, D. A. Rahn, M. Ramos, and D. Figueroa, 2011:
733 VOCALS-CUpEx: the Chilean Upwelling Experiment. *Atmos. Chem. Phys*, **11**, 2015-2029,
734 doi:10.5194/acp-11-2015-2011.
735 Garreaud, R. D., J. Rutllant, J. Quintana, J. Carrasco, and P. Minnis, 2001: CIMAR-5: A
736 snapshot of the lower atmosphere over the subtropical Southeast Pacific. *B. Am. Meteor.*
737 *Soc*., **82**. 2193-2207.
738 George, R. C., and R. Wood, 2010: Subseasonal variability of low cloud radiative properties over
739 the southeast Pacific Ocean. *Atmos. Chem. Phys.*, **10**, 4047-4063, doi:10.5194/acp-10-4047-
740 2010.
741 George, R. C., R. Wood, C. S. Bretherton, and G. Painter, 2013: Development and impact of
742 hooks of high droplet concentration on remote southeast Pacific stratocumulus. Submitted to
743 *Atmos. Chem. Phys.*, December 2012.
744 Grados, C., A. Chaigneau, K. Takahashi, B. Dewitte, R. Garreaud, and L. Gallardo, 2010:
745 VOCALS-REx Coastal Component/Componente Costera de VOCALS-REx. *CLIVAR-*
746 *Exchanges*, 15(**1**), 23-28.

747 Grell, G. A., Peckham, S. E., Schmitz, R., McKeen, S. A., Frost, G., Skamarock, W. C., and Eder,
748 B., 2005: Fully coupled ”online” chemistry within the WRF model, *Atmos. Environ.*, **39**,
749 6957–6975, doi:10.1016/j.atmosenv.2005.04.027.
750 Hawkins, L. N., L. M. Russell, D. S. Covert, P. K. Quinn, and T. S. Bates, 2010: Carboxylic
751 acids, sulfates, and organosulfates in processed continental organic aerosol over the
752 southeast Pacific Ocean during VOCALS-REx 2008. *J. Geophys. Res.*, **115**, D13201,
753 doi:10.1029/2009JD013276.
754 Holte, J. F. Straneo, C. Moffat, R. A. Weller, and J. T. Farrar, 2012: Structure and surface
755 properties of eddies in the Southeast Pacific Ocean. *J. Geophys. Res*. Submitted
756 Hoppel, W. A., G. M. Frick, and R. E. Larson, 1986: Effect of Nonprecipitating Clouds on the
757 Aerosol Size Distribution in the Marine Boundary-Layer, *Geophys. Res. Lett*, **13**, 125-128.
758 Huneeus, N., L. Gallardo and J. A. Rutllant, 2006: Offshore transport episodes of anthropogenic
759 sulfur in northern Chile: Potential impact on the stratocumulus deck. *Geophys. Res. Lett*., **33**.
760 doi: 10.1029/2006GL026921.
761 Jones, C., C. S. Bretherton, and D. Leon, 2011: Coupled vs. decoupled boundary layers in
762 VOCALS-REx. *Atmos. Chem. Phys.*, **11**, 7143-7153, doi:10.5194/acp-11-7143-2011.
763 Kazil, J., H. Wang, G. Feingold, A. D. Clarke, J. R. Snider, and A. R. Bandy, 2011: Modeling
764 chemical and aerosol processes in the transition from closed to open cells during VOCALS-
765 REx. *Atmos. Chem. Phys*., **11**, 7491-7514.
766 Klein, S.A., and D.L. Hartmann, 1993: The seasonal cycle of low stratiform clouds. *J. Climate*, **6**,
767 1587-1606.
768 Leon, D. C., Z. Wang, and D. Liu, 2008: Climatology of drizzle in marine boundary layer clouds
769 based on 1 year of data from CloudSat and Cloud-Aerosol Lidar and Infrared Pathfinder

Satellite Observations (CALIPSO). *J. Geophys. Res.*, **113**, D00A14, doi:10.1029/2008JD009835.

Lohmann, U. and Feichter, J.: Global indirect aerosol effects: a review, Atmos. Chem. Phys., 5, 715-737, doi:10.5194/acp-5-715-2005, 2005.

Ma, C.-C., C. R. Mechoso, A. W. Robertson and A. Arakawa, 1996: Peruvian stratus clouds and the tropical Pacific circulation - a coupled ocean-atmosphere GCM study. *J. Climate*, 9, 1635-1645.

Mechem, D. B., S. E. Yuter, and S. P. de Szoeke, 2012:Thermodynamic and aerosol controls in southeast Pacific stratocumulus. *J. Atmos. Sci.,* **69**, 1250-1266

Mechoso, C. R., A. W. Robertson, N. Barth, M. K. Davey, P. Delecluse, P. R. Gent, S. Ineson, B. Kirtman, M. Latif, H. Le Treut, T. Nagai, J. D. Neelin, S. G. H. Philander, J. Polcher, P. S. Schopf, T. Stockdale, M. J. Suarez, L. Terray, O. Thual and J. J. Tribbia, 1995: The seasonal cycle over the Tropical Pacific in General Circulation Models. *Mon. Wea. Rev*., **123**, 2825-2838.

Mechoso, C. R. and R. Wood, 2010: An abbreviated history of VOCALS. *CLIVAR Exchanges*, 53, April 2010.

Min, Q., Joseph, E., Lin, Y., Min, L., Yin, B., Daum, P. H., Kleinman, L. I., Wang, J., and Lee, Y.-N.: Comparison of MODIS cloud microphysical properties with in-situ measurements over the Southeast Pacific, *Atmos. Chem. Phys.*, **12**, 11261-11273, doi:10.5194/acp-12-11261-2012, 2012

O'Dell, C.W., F. J. Wentz, and R. Bennartz, 2008. Cloud liquid water path from satellite-based passive microwave observations: a new climatology over the global oceans. *J. Climate,* **21**, 1721–1739.

793 Painemal, D., R. Garreaud, J. Rutllant, and P. Zuidema, 2010: Southeast Pacific stratus: High
794 frequency variability and meso-scale structures over San Felix Island. *J. Appl. Meteor. Clim.*
795 **49**, pp. 463-477.
796 Painemal, D. and P. Zuidema, 2010: Microphysical variability in Southeast Pacific
797 stratocumulus clouds: Synoptic conditions and radiative response. *Atmos. Chem. Phys.*,
798 **10**, pp. 6255-6269.
799 Painemal, D. and P. Zuidema, 2011: Assessment of MODIS cloud effective radius and optical
800 thickness retrievals over the Southeast Pacific with VOCALS-REx in-situ measurements.
801 *J. Geophys. Res.*, **116**, D24206, doi:10.1029/2011JD016155
802 Painter, G., 2012: A Lagrangian Study of Southeast Pacific Boundary Layer Clouds. M. S.
803 Thesis, Dept. of Atmos. Sci., Univ. Washington, 48 pp.
804 Petters, M. D., J. R. Snider, B. Stevens, G. Vali, I. Faloona, and L. Russell, 2006: Accumulation
805 mode aerosol, pockets of open cells, and particle nucleation in the remote subtropical Pacific
806 marine boundary layer. *J. Geophys. Res.*, **111**, D02206, doi:10.1029/2004JD005694.
807 Philander, S.G.H., D. Gu, D. Halpern, G. Lambert, N.C. Lau, T. Li and R.C. Pacanowski, 1996:
808 Why the ITCZ is mostly north of the equator, *J. Climate*, **9**, 2958-2972.
809 Quaas, J., Y. Ming, S. Menon, T. Takemura, M. Wang, J. E. Penner, A. Gettelman, U. Lohmann,
810 N. Bellouin, O. Boucher, A. M. Sayer, G. E. Thomas, A. McComiskey, G. Feingold, C.
811 Hoose, J. E. Kristjánsson,, X. Liu, Y. Balkanski, L. J. Donner, P. A. Ginoux, P. Stier, B.
812 Grandey, J. Feichter, I. Sednev, S. E. Bauer, D. Koch, R. G. Grainger, A. Kirkevåg, T.
813 Iversen, Ø. Seland, R. Easter, S. J. Ghan, P. J. Rasch, H. Morrison, J. –F. Lamarque, M. J.
814 Iacono, S. Kinne, and M. Schulz, 2009: Aerosol indirect effects – general circulation model

intercomparison and evaluation with satellite data. *Atmos. Chem. Phys.*, **9**, 8697-8717, doi:10.5194/acp-9-8697-2009.

Rahn, D., and R. Garreaud, 2010a: Marine boundary layer over the subtropical southeast Pacific during VOCALS-REx. Part I: Mean structure and diurnal cycle. *Atmos. Chem. Phys.*, **10**, 4047-4063.

Rahn, D., and R. Garreaud, 2010b: Marine boundary layer over the subtropical southeast Pacific during VOCALS-REx. Part II: Synoptic variability. *Atmos. Chem. Phys.,* **10**, 4491-4505

Rahn, D., R. Garreaud and J. Rutllant, 2011: The low-level atmospheric circulation near Tongoy Bay point Lengua de Vaca (Chilean coast, 30°S). *Mon. Wea. Rev.* **139**. 3628-3647.

Rosenfeld, D., Kaufman, Y. J., and Koren, I., 2006: Switching cloud cover and dynamical regimes from open to closed Benard cells in response to the suppression of precipitation by aerosols, *Atmos. Chem. Phys*., **6**, 2503-2511, doi:10.5194/acp-6-2503-2006.

Rutllant, J. A., R. C. Muñoz, and R. D. Garreaud, 2012: Meteorological observations in the Northern Chilean coast during VOCALS-REx, *Atmos. Chem. Phys.* Discuss., **12**, 22783-22811, doi:10.5194/acpd-12-22783-2012.

Saide, P. E., S. N. Spak, G. R. Carmichael, M. A. Mena-Carrasco, Q. Yang, S. Howell, D. C. Leon, J. R. Snider, A. R. Bandy, J. L. Collett, K. B. Benedict, S. P. de Szoeke, L. N. Hawkins, G. Allen, I. Crawford, J. Crosier, and S. R. Springston, 2012a: Evaluating WRF-Chem aerosol indirect effects in Southeast Pacific marine stratocumulus during VOCALS-REx. *Atmos. Chem. Phys.*, **12**, 3045-3064.

Saide, P. E., G. R. Carmichael, S. N. Spak, P. Minnis, and J. K. Ayers, 2012b: Improving aerosol distributions below clouds by assimilating satellite-retrieved cloud droplet number. *Proc. Nat. Acad. Sci*., **109**, 11939-11943.

838 Savic-Jovcic, V. and B. Stevens, 2008: The structure and mesoscale organization of precipitating
839 stratocumulus, *J. Atmos. Sci.,* **65**, 1587-1605.

840 Schneider, W., R. Fuenzalida, E. Rodríguez-Rubio, and J. Garcés-Vargas, 2003: Characteristics
841 and formation of Eastern South Pacific Intermediate Water. *Geophys. Res. Lett*., **30**, NO. 11,
842 1581, doi:10.1029/2003GL017086.

843 Serpetzoglou, E., B. Albrecht, P. Kollias, and C. Fairall, 2008: Boundary layer, cloud, and
844 drizzle variability in the southeast Pacific stratocumulus regime. *J. Clim*., **21**, p. 6191-6214.

845 Shank, L. M., S. Howell, A. D. Clarke, S. Freitag, V. Brekhovskikh, V. Kapustin, C.
846 McNaughton, T. Campos, and R. Wood, 2011: Organic carbon and non-refractory aerosol
847 over the remote Southeast Pacific: oceanic and combustion sources. *Atmos. Chem. Phys.*
848 *Discuss.,* **11**, 16895-16932, doi:10.5194/acpd-11-16895-2011.

849 Sharon, T. M., B. A. Albrecht, H. H. Johnson, P. Minnis, M. M. Khaiyer, T. Van Reken, J.
850 Seinfeld, and R. Flagan, 2005: Aerosol and cloud microphysical characteristics of rifts and
851 gradients in maritime stratocumulus clouds. Accepted, *J. Atmos. Sci.*, **63**, 983-997.

852 Stevens, B., G. Vali, K. Comstock, R. Wood, M. VanZanten, P. H. Austin, C. S. Bretherton, D.
853 H. Lenschow, 2005: Pockets of Open Cells (POCs) and Drizzle in Marine Stratocumulus.
854 *Bull. Am. Meteorol. Soc.,* **86**, 51-57.

855 Sun, F., A. Hall, and X. Qu, 2011: On the relationship between low cloud variability and lower
856 tropospheric stability in the Southeast Pacific. *Atmos. Chem. Phys.*, **11**, 9053-9065.

857 Sun, R., S. Moorthi, H. Xiao, and C. R. Mechoso, 2010: Simulation of low clouds in the
858 Southeast Pacific by the NCEP GFS: sensitivity to vertical mixing, *Atmos. Chem. Phys*., **10**,
859 12261-12272, doi: 10.5194/acp-10-12261-2010.

Terai, C. R., R. Wood, D. C. Leon, and P. Zuidema, 2012: Does precipitation susceptibility vary with increasing cloud thickness in marine stratocumulus? *Atmos. Chem. Phys.,* **12**, 4567-4583, doi:10.5194/acp-12-4567-2012.

Tomlinson, J. M., Li, R., and Collins, D. R. 2007: Physical and chemical properties of the aerosol within the Southeastern Pacific marine boundary layer, *J. Geophys. Res.,* **112**, D12211, doi:10.1029/2006JD007771..

Toniazzo, T., C. R. Mechoso, L. Shaffrey, and J. M. Slingo, 2009: Upper ocean heat budget and ocean eddy transport in the South-East Pacific in a high resolution coupled model. *Clim. Dyn*. doi 10.1007/s00382-009-0703-8.

Toniazzo, T., S. J. Abel, R. Wood, C. R. Mechoso, L. C. Shaffrey, 2011: Large-scale and synoptic meteorology in the south-east Pacific during the observations campaign VOCALS-REx in Spring 2008. Submitted to *Atmos. Chem. Phys.*, **11**, 5237-5262, doi:10.5194/acp-11-5237-2011.

Toniazzo, T., F. Sun, C. R. Mechoso, and A. Hall, 2012: A regional modeling study of the diurnal cycle in the lower troposphere in the southeastern tropical Pacific. *Clim. Dyn*,

Twomey, S., 1974: Pollution and the planetary albedo. *Atmos. Environ.* **8**, 1251–6.

Twomey, S., 1977: The Influence of Pollution on the Shortwave Albedo of Clouds". *J. Atmos. Sci.* **34**, 1149–52.

Twohy, C. H., J. Anderson, D. Toohey, M. Andrejczuk, A. Adams, M. Lytle, R. George, R. Wood, P. Saide, S. Spak, P. Zuidema and D. Leon, 2012: Impacts of aerosol particles on the microphysical and radiative properties of stratocumulus clouds over the Southeast Pacific ocean. *Atmos. Chem. Phys. Discuss.*, **12**, pp. 19715-19767. doi:10.5194/acpd-12-19715-2012.

883 UNEP, 2009. Sherman, K., and G. Hempel (Editors): The UNEP Large Marine Ecosystem
884 Report. A perspective on changing conditions in LMEs of the world's regional seas. UNEP
885 Regional Seas Report and Studies No. 182. The United Nations Environment Program.
886 Nairobi, Kenya.

887 VanZanten, M. C., and B. Stevens, 2005: Observations of the structure of heavily precipitating
888 marine stratocumulus, *J. Atmos. Sci.*, **62**, 4327–4342.

889 Waliser, D. E., M. Moncrieff, D. Burrridge, Andreas H. Fink, D. Gochis, B. N. Goswami, B.
890 Guan, P. Harr, J. Heming, H.-H. Hsu, C. Jakob, M. Janiga, R. Johnson, S. Jones, P.
891 Knippertz, J. Marengo, H. Nguyen, M. Pope, Y. Serra, C. Thorncroft, M. Wheeler, R. Wood,
892 S. E. Yuter, 2012: The "Year" of Tropical Convection (May 2008 to April 2010): Climate
893 Variability and Weather Highlights. *Bull. Amer. Meteorol. Soc.*,
894 http://dx.doi.org/10.1175/2011BAMS3095.1, August 2012.

895 Wang H., and G. Feingold, 2009a: Modeling mesoscale cellular structures and drizzle in marine
896 stratocumulus. Part 1: Impact of drizzle on the formation and evolution of open cells. *J.*
897 *Atmos. Sci.*, **66**, 3237 - 3256.

898 Wang H., and G. Feingold, 2009b: Modeling mesoscale cellular structure and drizzle in marine
899 stratocumulus. Part 2: The microphysics and dynamics of the boundary region between open
900 and closed cells. *J. Atmos. Sci.*, **66**, 3257 - 3275.

901 Wang, H., Feingold, G., Wood, R., and Kazil, J., 2010: Modelling microphysical and
902 meteorological controls on precipitation and cloud cellular structures in Southeast Pacific
903 stratocumulus. *Atmos. Chem. Phys.*, **10**, 6347-6362, doi:10.5194/acp-10-6347-2010.

Wang, S., L. W. O'Neill, Q. Jiang, S. P. de Szoeke, X. Hong, H. Jin, W. T. Thompson, and and X. Zheng, 2011: A regional real-time forecast of marine boundary layers during VOCALS-Rex. *Atmos. Chem. Phys.*, **11**, 421-437.

Whelan, S. P. J. Lord, N. Galbraith, R. Weller, J. T. Farrar, D. Grant, C. Grados, S. P. de Szoeke, C. Moffat, C. Zappa, M. Yang. F. Straneo, C. Fairall, P. Zuidema, D. Wolkfe, M. Miller, and D. Covert, 2009. Stratus 9/VOCALS Ninth Setting of the Stratus Ocean Reference Station& VOCALS Regional Experiment. Cruise RB-08-06 September 29–December 2, 2008 Leg 1: Charleston–Arica, September 29–November 3, 2008 Leg 2: Arica–Arica, November 9–December 2, 2008. Woods Hole Oceanographic Institution Technical Report WHOI-2009-03; UOP Technical Report 2009-02, 127 pp.

Wood, R., and C. S. Bretherton, 2004: Boundary layer depth, entrainment and decoupling in the cloud-capped subtropical and tropical marine boundary layer. *J. Clim*., **17**, 3576-3588.

Wood, R. and D. L. Hartmann, 2006: Spatial variability of liquid water path in marine boundary layer clouds: The importance of mesoscale cellular convection. *J. Climate,* **19**, 1748–1764.

Wood, R., M. Köhler, R. Bennartz, and C. O'Dell, 2009: The diurnal cycle of surface divergence over the global oceans. *Quart. J. Roy. Meteorol. Soc*., **135,** 1484-1493, 2009

Wood, R., K. K. Comstock, C. S. Bretherton, J. Tomlinson, and C. Fairall, 2008: Open cellular structure in marine stratocumulus sheets. *J. Geophys. Res.,* **113**, D12207, doi:10.1029/2007JD009371.

Wood, R., C. R. Mechoso, C. S. Bretherton, R. A. Weller, B. Huebert, F. Straneo, B. A. Albrecht, H. Coe, G. Allen, G. Vaughan, P. Daum, C. Fairall, D. Chand, L. Gallardo Klenner, R. Garreaud, C. Grados Quispe, D. S. Covert, T. S. Bates, R. Krejci, L. M. Russell, S. de Szoeke, A. Brewer, S. E. Yuter, S. R. Springston, A. Chaigneau, T. Toniazzo, P. Minnis, R.

927 Palikonda, S. J. Abel, W. O. J. Brown, S. Williams, J. Fochesatto, J. Brioude, 2011a: The
928 VAMOS Ocean-Cloud-Atmosphere-Land Study Regional Experiment (VOCALS-REx):
929 goals, platforms, and field operations. *Atmos. Chem. Phys.*, **11**, 627-654.

930 Wood, R., C. S. Bretherton, D. Leon, A. D. Clarke, P. Zuidema, G. Allen, and H. Coe, 2011b:
931 An aircraft case study of the spatial transition from closed to open mesoscale cellular
932 convection over the Southeast Pacific. *Atmos. Chem. Phys*., **11**, 2341-2370.

933 Wood, R., D. Leon, M. Lebsock, J. Snider, and A. D. Clarke, 2012**:** Precipitation driving of
934 droplet concentration variability in marine low clouds**.** *J. Geophys. Res.,*

935 Wood, R., 2012: Stratocumulus Clouds. *Mon. Wea. Rev.*, **140**, 2373–2423.

936 Wyant, M. C., R. Wood, C. S. Bretherton, C. R. Mechoso, J. Bacmeister, M. A. Balmaseda, B.
937 Barrett, F. Codron, P. Earnshaw, J. Fast, C. Hannay, J. W. Kaiser, H. Kitagawa, S. A. Klein,
938 M. Köhler, J. Manganello, H. –L. Pan, F. Sun, S. Wang, and Y. Wang, 2010: The PreVOCA
939 experiment: modeling the lower troposphere in the Southeast Pacific. *Atmos. Chem. Phys*.,
940 **10**, 4757-4774, doi:10.5194/acp-10-4757-2010.

941 Yang, M. W. I. Gustafson Jr., J. D. Fast, H. Wang, R. C. Easter, H. Morrison, Y. -N. Lee, E. G.
942 Chapman, S. N. Spak, and M. A. Mena-Carrasco, 2011: Atmospheric sulfur cycling in the
943 southeastern Pacific - longitudinal distribution, vertical profile, and diurnal variability
944 observed during VOCALS-REx. *Atmos. Chem. Phys.*, **11**, pp. 5079-5097. doi:10.5194/acp-
945 11/5079-2011.

946 Yang, Q., W. I. Gustafson Jr., J. D. Fast, H. Wang, R. C. Easter, H. Morrison, Y. -N. Lee, E. G.
947 Chapman, S. N. Spak, and M. A. Mena-Carrasco, 2011: Assessing regional scale predictions
948 of aerosols, marine stratocumulus, and their interactions during VOCALS-REx using WRF-
949 Chem. *Atmos. Chem. Phys*., **11**, 11951-11975.

Yu, J.-Y., and C. R. Mechoso, 1999a: A discussion on the errors in the surface heat fluxes simulated by a coupled GCM. *J. Climate*, **12**, 416-426.

Yu, J.-Y., and C. R. Mechoso, 1999b: Links between annual variations of Peruvian stratus clouds and of SST in the eastern equatorial Pacific. *J. Climate*, **12**, 3,305-3,318.

Zhang, M. H., and Coauthors, 2005: Comparing clouds and their seasonal variations in 10 atmospheric general circulation models with satellite measurements. *J. Geophys. Res.,* **110,** D15S02, doi:10.1029/2004JD005021.

Zheng J., T. Shinoda, J. L. Lin, and G. N. Kiladis, 2011: Sea surface temperature biases under the stratus cloud deck in the Southeast Pacific ocean in 19 IPCC AR4 coupled general circulation models. *J Clim*. doi:10.1175/2011JCLI4172.1

Zheng, J., T. Shinoda, G. N. Kiladis, J. Lin, E. J. Metzger, H. E. Hurlburt, and B. S. Giese, 2010: Upper-ocean processes under the stratus cloud deck in the Southeast Pacific Ocean. *J. Phys. Oceanogr*., 40:103\u2013120. doi:10.1175/2009JPO4213.1

Zheng, X., 2011: A regional real-time forecast of marine boundary layers during VOCALS-REx, *Atmos. Chem. Phys.*, **11**, 421-437, doi:10.5194/acp-11-421-2011.

Zheng, X., B. Albrecht, H. H. Jonsson, D. Khelif, G. Feingold, P. Minnis, K. Ayers, P. Chuang, S. Donaher, D. Rossiter, V. Ghate, J. Ruiz-Plancarte, and S. Sun-Mack, 2011: Observations of the boundary layer, cloud, and aerosol variability in the southeast Pacific near-coastal marine stratocumulus during VOCALS-REx, *Atmos. Chem. Phys*., **11**, 9943-9959, doi:10.5194/acp-11-9943-2011.

Zuidema, P., D. Painemal, S. deSzoeke and C. Fairall, 2009: Stratocumulus cloud top height estimates and their climatic implications. *J. Clim.*, **22**, pp. 4652-4666.

Zuidema, P. D. Leon, A. Pazmany and M. Cadeddu, 2012: Aircraft millimeter-wave passive sensing of cloud liquid water and water vapor during VOCALS-REx. *Atmos. Chem. Phys.*, **12**, pp. 355-369, doi:10.5194/acp-12-355-2012.

Figure Captions

Figure 1. The VOCALS study region

Figure 2. The first ten years (2001-2010) of upper ocean temperature data from the WHOI buoy, daily averaged and contoured and with two mixed layer depth estimates, the white line showing where temperature is 0.5°C cooler than the surface and the black line showing when temperature is 1.0°C cooler than the surface.

Figure 3. Schematics of the VOCALS-Regional Experiment (REx)

Figure 4. Concentrations along 20°S of (a) cloud droplet number and (b) sulfate mass at 150 m altitude from assorted VOCA models and C-130 observations.

Figure 5. Surface heat budget errors of CGCMs participating in CMIP3. Surface heat budget errors of CGCMs participating in CMIP3. The latent heat flux error is largest, damping warm SST errors. The ocean residual error is on the order of the radiative error, but less consistent among models. Surface fluxes measured along 20°S imply the southeastern Pacific Ocean circulation plays an important role in the upper ocean heat budget, and that these circulations are often improperly simulated in CGCMs.

Figure 6. Alongshore absolute geostrophic velocity (m/s) near the Perú shelf (14°S) in 2008: (a) October 4th-8th, (b) October 18th-22th, and (c) November 3rd-8th . See Pietri et al. (2012) for more details on the data.

Figure 7. Cloud, precipitation and aerosol mean statistics taken along the 20°S cross section. (a) cloud top, base and LCL from the VOCALS ship cruises and from the C-130 during REx; (b) cloud fraction (blue) and liquid water path (LWP, black) from the C-130, from the ship cruises,

997 and from passive microwave satellite (AMSR-E) during REx; (c) Precipitation rate estimates
998 from four instruments on three platforms: RHB C-band
999 scanning radar (black circles), CloudSat cloud radar (red line), C-130 aircraft zenith and nadir-
1000 pointing cloud radar (black squares), and the C-130 2D-C drop probe (blue squares). Error bars
1001 show estimated uncertainties. Radar cloud base rain rates are derived from the maximum
1002 reflectivity in each boundary layer column sampled; (d) Near-surface aerosol concentrations for
1003 particles larger than 0.1 μm (black) from the RHB and the aircraft (Allen et al. 2011) and cloud
1004 droplet concentrations (red) from aircraft and from MODIS (Bretherton et al. 2010); (e)
1005 submicron sulfate aerosol mass loadings from the RHB and from the aircraft in REx; (f)
1006 schematic summarizing the key aerosol, cloud and precipitation changes from the coast to the
1007 remote ocean along 20°S.
1008 Figure 9. a) RF05 (10/26/2008) flight track over 20S color coded with measured CO and
1009 illustrating patchy CO layers above the indicated inversion and higher altitude CO layers east
1010 and west of 78W. Lowest CO evident in MBL west of 80W is still frequently higher that typical
1011 clean air advected from south into the VOCALS region. b) size distributions for above cloud legs
1012 west of 78W are shown relative to the position of Hopple minimum (indicating MBL CCN are
1013 larger than about 50 nm) commonly observed in the MBL. c) Number larger than 50 nm
1014 integrated from size distributions (Ngt50) vs. black carbon mass (SP2 Inc. Mass) and color coded
1015 by CO concentrations.
1016

Figures

Click here to download Manuscript: BAMS_Figures_Mechoso.docx

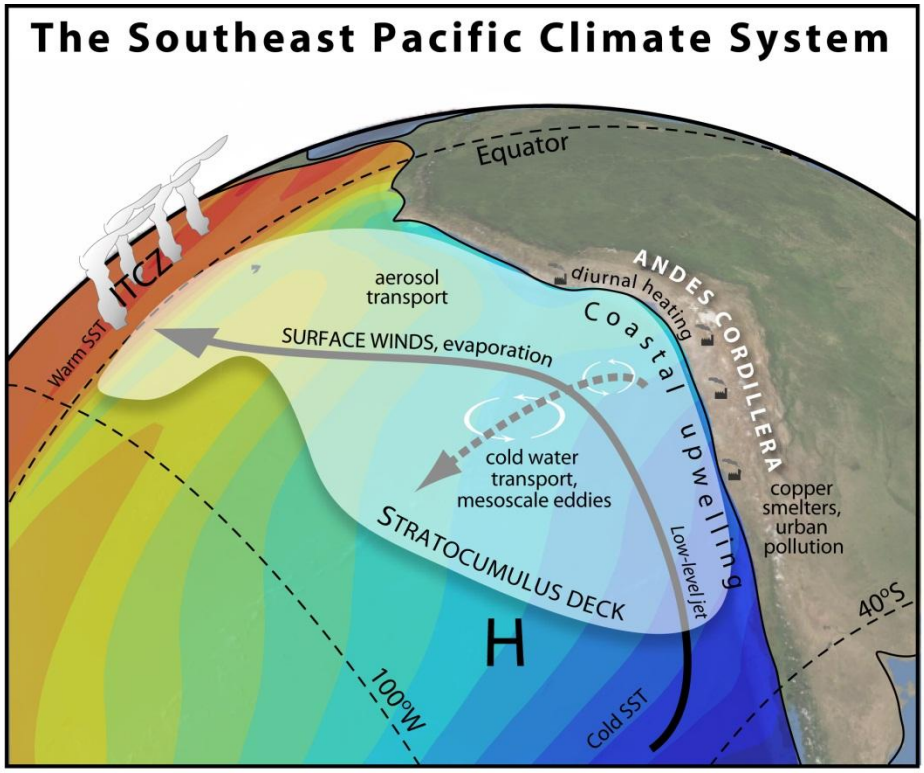

Figure 1. The VOCALS study region

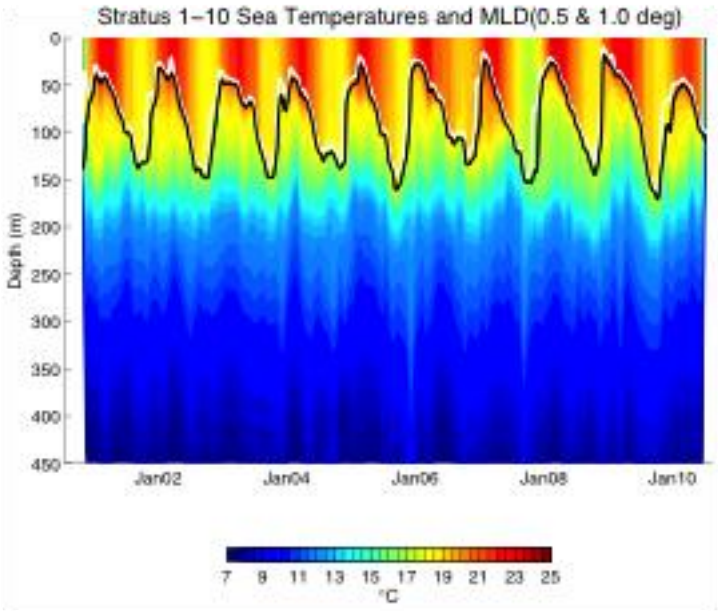

Figure 2. The first ten years (2001-2010) of upper ocean temperature data from the WHOI buoy, daily averaged and contoured and with two mixed layer depth estimates, the white line showing where temperature is 0.5°C cooler than the surface and the black line showing when temperature is 1.0°C cooler than the surface.

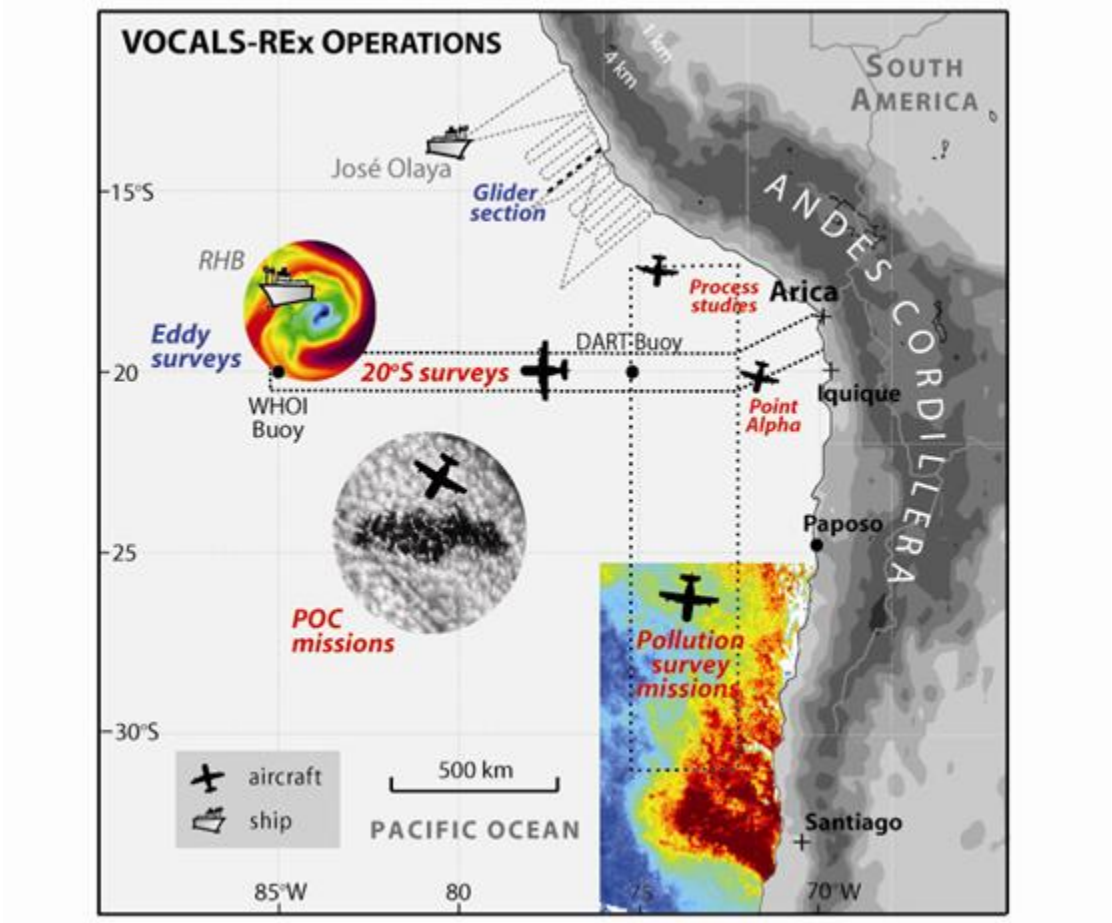

Figure 3. Schematics of the VOCALS-Regional Experiment (REx)

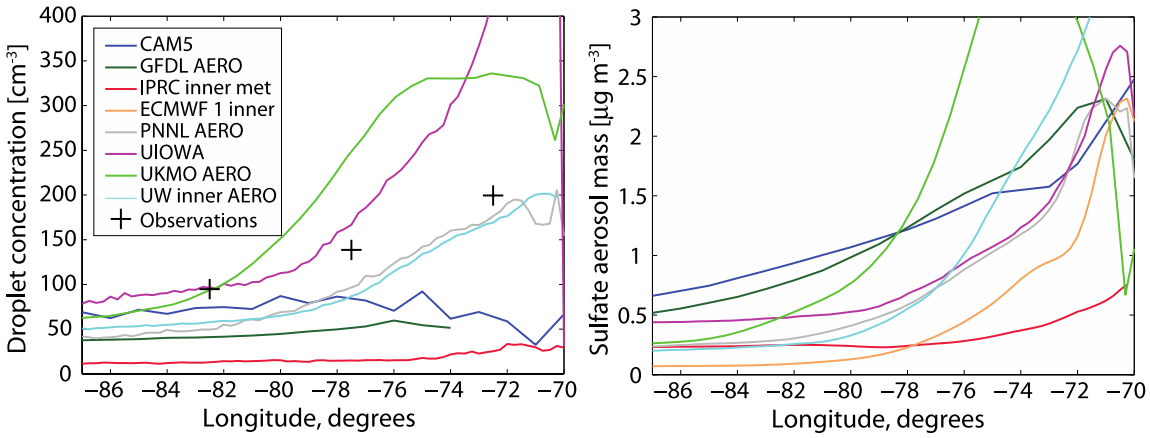

Figure 4. Concentrations along 20°S of (a) cloud droplet number and (b) sulfate mass at 150 m altitude from assorted VOCA models and C-130 observations

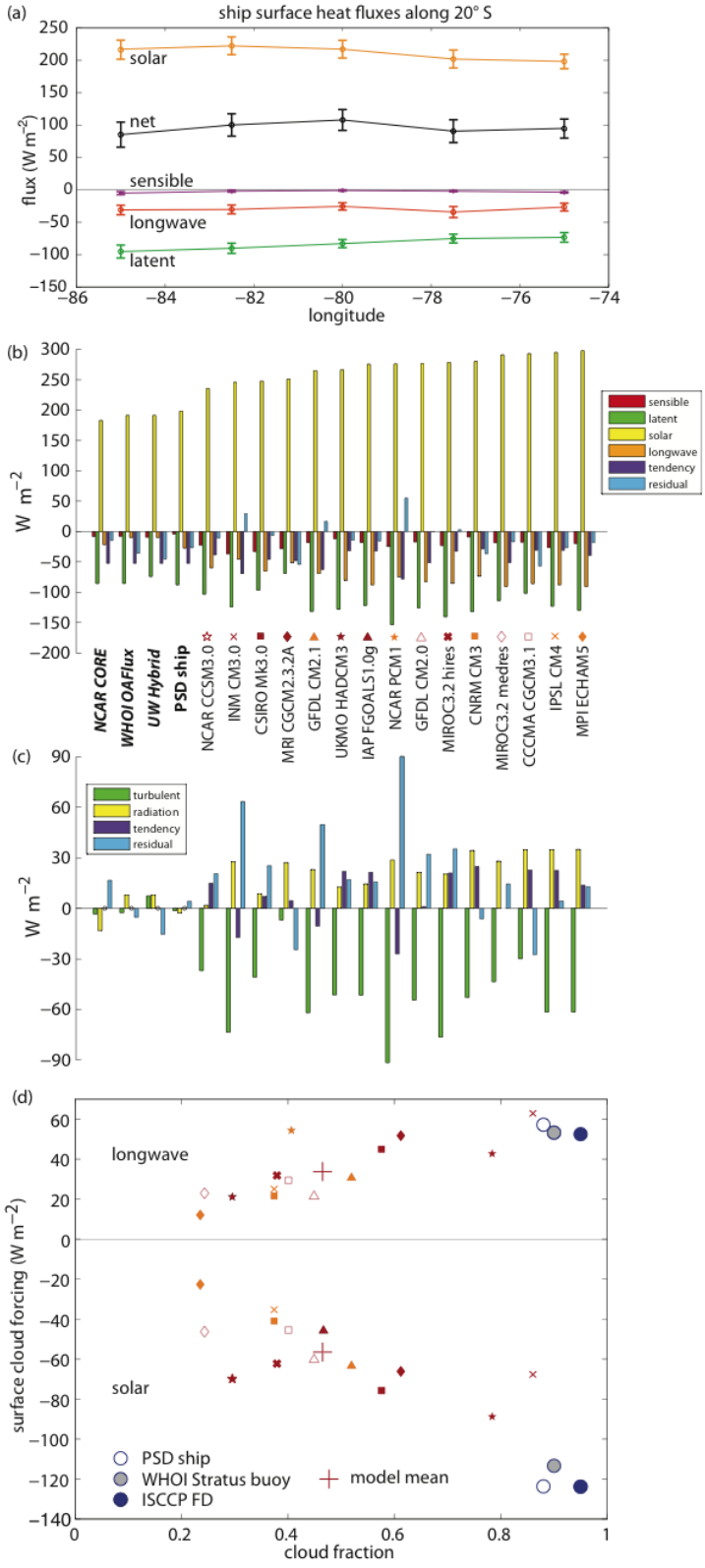

Figure 5. Surface heat budget errors of CGCMs participating in CMIP3. Surface heat budget errors of CGCMs participating in CMIP3. The latent heat flux error is largest, damping warm SST errors. The ocean residual error is on the order of the radiative error, but less consistent among models. Surface fluxes measured along 20°S imply the southeastern Pacific Ocean circulation plays an important role in the upper ocean heat budget, and that these circulations are often improperly simulated in CGCMs.

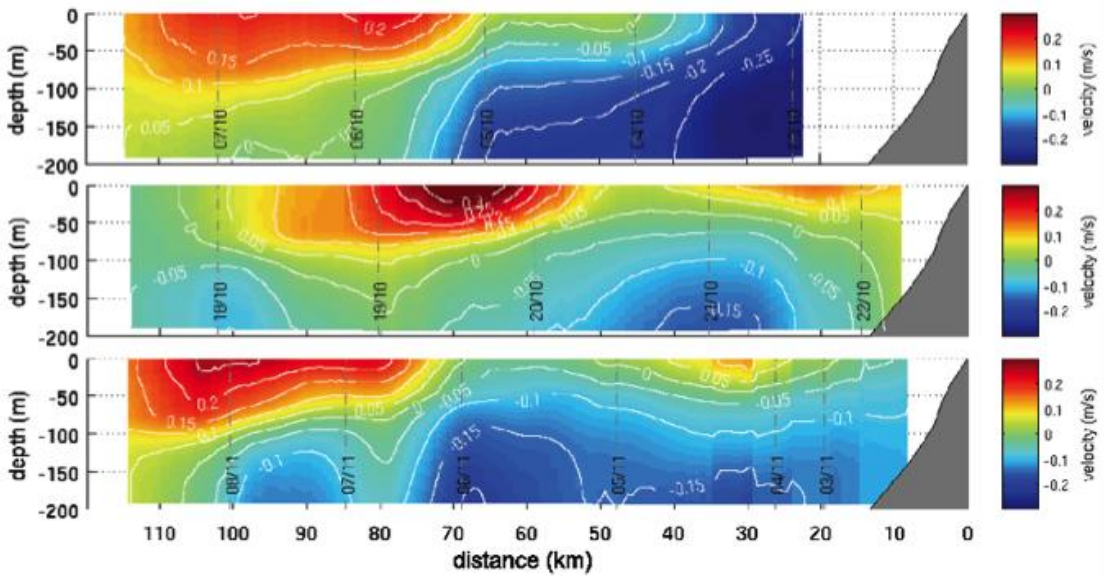

Figure 6. Alongshore absolute geostrophic velocity (m/s) near the Perú shelf (14°S) in 2008: (a) October 4th-8th, (b) October 18th-22th, and (c) November 3rd-8th. See Pietri et al. (2012) for more details on the data.

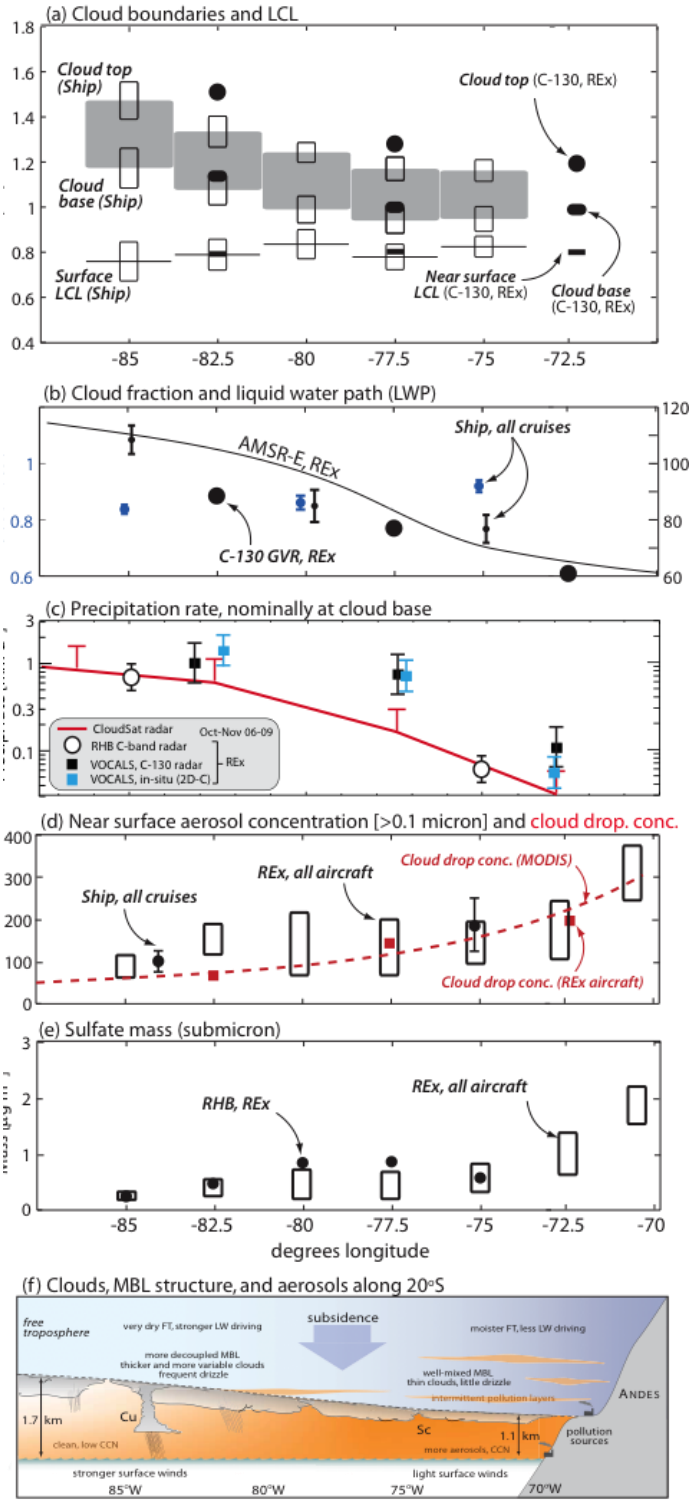

Figure 7. Cloud, precipitation and aerosol mean statistics taken along the 20°S cross section. (a) cloud top, base and LCL from the VOCALS ship cruises and from the C-130 during REx; (b) cloud fraction (blue) and liquid water path (LWP, black) from the C-130, from the ship cruises, and from passive microwave satellite (AMSR-E) during REx; (c) Precipitation rate estimates from four instruments on three platforms: RHB C-band scanning radar (black circles), CloudSat cloud radar (red line), C-130 aircraft zenith and nadir-pointing cloud radar (black squares), and the C-130 2D-C drop probe (blue squares). Error bars show estimated uncertainties. Radar cloud base rain rates are derived from the maximum reflectivity in each boundary layer column sampled; (d) Near-surface aerosol concentrations for particles larger than 0.1 μm (black) from the RHB and the aircraft (Allen et al. 2011) and cloud droplet concentrations (red) from aircraft and from MODIS (Bretherton et al. 2010); (e) submicron sulfate aerosol mass loadings from the RHB and from the aircraft in REx; (f) schematic summarizing the key aerosol, cloud and precipitation changes from the coast to the remote ocean along 20°S.

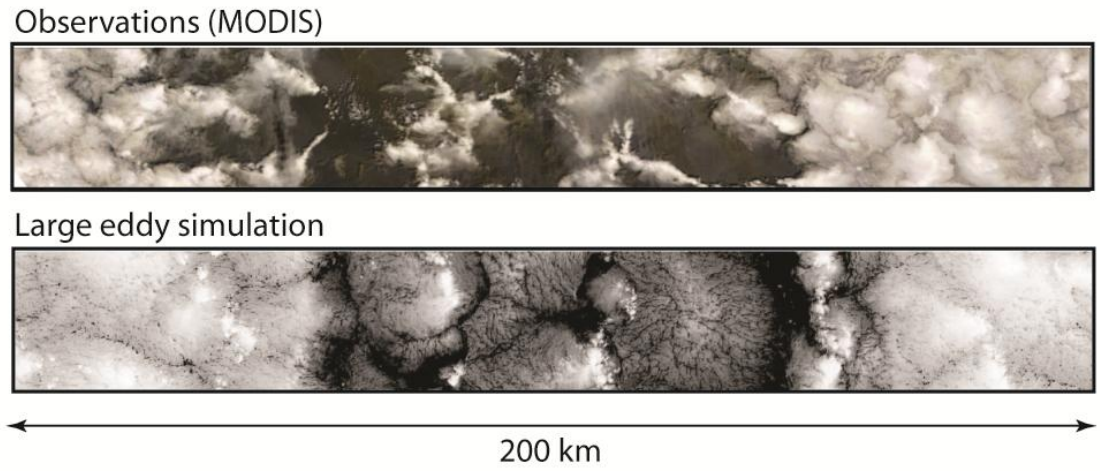

Figure 8. Comparison of satellite-observed (top) and modeled (bottom) Pocket of Open Cells (POC) sampled during VOCALS-REx on 28th October 2008.

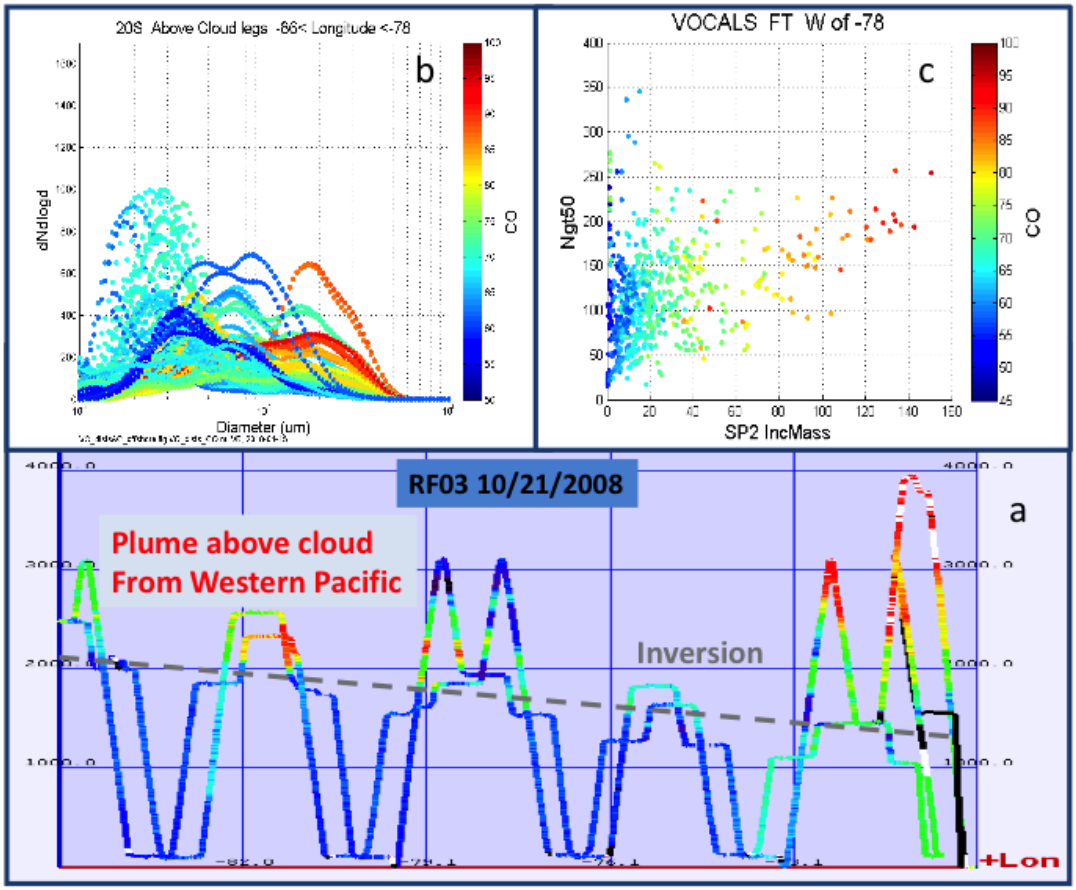

Figure 9. a) RF05 (10/26/2008) flight track over 20S color coded with measured CO and illustrating patchy CO layers above the indicated inversion and higher altitude CO layers east and west of 78W. Lowest CO evident in MBL west of 80W is still frequently higher that typical clean air advected from south into the VOCALS region. b) size distributions for above cloud legs west of 78W are shown relative to the position of Hopple minimum (indicating MBL CCN are larger than about 50 nm) commonly observed in the MBL. c) Number larger than 50 nm integrated from size distributions (Ngt50) vs. black carbon mass (SP2 Inc. Mass) and color coded by CO concentrations.